Technology Collaboration Programme
by IEA

International Energy Agency
Photovoltaic Power Systems Programme

Task 13 Reliability and Performance of Photovoltaic Systems

PVPS

Best Practices for the Optimization of Bifacial Photovoltaic Tracking Systems

2024

Report IEA-PVPS T13-26:2024

What is IEA PVPS TCP?

The International Energy Agency (IEA), founded in 1974, is an autonomous body within the framework of the Organization for Economic Cooperation and Development (OECD). The Technology Collaboration Programme (TCP) was created with a belief that the future of energy security and sustainability starts with global collaboration. The programmes are made up of 6,000 experts across government, academia, and industry dedicated to advancing common research and the application of specific energy technologies.

The IEA Photovoltaic Power Systems Programme (IEA PVPS) is one of the TCP's within the IEA and was established in 1993. The mission of the programme is to "enhance the international collaborative efforts which facilitate the role of photovoltaic solar energy as a cornerstone in the transition to sustainable energy systems." In order to achieve this, the Programme's participants have undertaken a variety of joint research projects in PV power systems applications. The overall programme is headed by an Executive Committee, comprised of one delegate from each country or organisation member, which designates distinct 'Tasks,' that may be research projects or activity areas.

The 25 IEA PVPS participating countries are Australia, Austria, Belgium, Canada, China, Denmark, Finland, France, Germany, Israel, Italy, Japan, Korea, Malaysia, Morocco, the Netherlands, Norway, Portugal, South Africa, Spain, Sweden, Switzerland, Thailand, Turkey, and the United States of America. The European Commission, Solar Power Europe, the Smart Electric Power Alliance, the Solar Energy Industries Association, the Solar Energy Research Institute of Singapore and Enercity SA are also members.

Visit us at: www.iea-pvps.org

What is IEA PVPS Task 13?

Within the framework of IEA PVPS, Task 13 aims to provide support to market actors working to improve the operation, the reliability and the quality of PV components and systems. Operational data from PV systems in different climate zones compiled within the project will help provide the basis for estimates of the current situation regarding PV reliability and performance.

The general setting of Task 13 provides a common platform to summarize and report on technical aspects affecting the quality, performance, reliability and lifetime of PV systems in a wide variety of environments and applications. By working together across national boundaries, we can all take advantage of research and experience from each member country and combine and integrate this knowledge into valuable summaries of best practices and methods for ensuring PV systems perform at their optimum and continue to provide competitive return on investment.

Task 13 has so far managed to create the right framework for the calculations of various parameters that can give an indication of the quality of PV components and systems. The framework is now there and can be used by the industry who has expressed appreciation towards the results included in the high-quality reports.

The IEA PVPS countries participating in Task 13 are Australia, Austria, Belgium, Canada, Chile, China, Denmark, Finland, France, Germany, Israel, Italy, Japan, the Netherlands, Norway, Spain, Sweden, Switzerland, Thailand, and the United States of America.

COVER PICTURE

Photovoltaic bifacial single-axis tracker power plant. Courtesy of European Energy A/S.

ISBN 978-3-907281-62-8: Best Practices for the Optimization of Bifacial Photovoltaic Tracking Systems

INTERNATIONAL ENERGY AGENCY
PHOTOVOLTAIC POWER SYSTEMS PROGRAMME

Best Practices for the Optimization of Bifacial Photovoltaic Tracking Systems

IEA PVPS Task 13
Reliability and Performance of Photovoltaic Systems

Report IEA-PVPS T13-26:2024
August 2024

ISBN 978-3-907281-62-8

AUTHORS

Main Authors

Joshua S. Stein, Sandia National Laboratories, USA
Giosuè Maugeri, RSE, Italy
Nicholas Riedel-Lyngskær, European Energy, Denmark
Silvana Ovaitt, National Renewable Energy Laboratory, USA
Thore Müller, PVRADAR Labs, Germany
Shuo Wang, TUAS, Finland
Hugo Huerta, TUAS, Finland
Jonathan Leloux, Lucisun, Belgium
Jan Vedde, European Energy, Denmark
Matthew Berwind, Fraunhofer ISE, Germany
Maddalena Bruno, Fraunhofer ISE, Germany
Daniel Riley, Sandia National Laboratories, USA
Ramesh Santhosh, IMEC, Belgium
Samuli Ranta, TUAS, Finland
Michael Green, Arava, Israel
Kevin Anderson, Sandia National Laboratories, USA
Lelia Deville, Sandia National Laboratories, USA

Editors

Joshua S. Stein, Sandia National Laboratories, USA
Ulrike Jahn, Fraunhofer CSP, Germany

TABLE OF CONTENTS

ACKNOWLEDGEMENTS

This paper received valuable contributions from many IEA-PVPS Task 13 members and other international experts. Many thanks to the experts that contributed to the two surveys and performance modeling comparison. We would like to acknowledge: Vicente Cortez and Akhil Johnson of McCarthy Building Companies, Inc for submitting modeling results.

Sandia National Laboratories is a multimission laboratory managed and operated by National Technology & Engineering Solutions of Sandia, LLC, a wholly owned subsidiary of Honeywell International Inc., for the U.S. Department of Energy's National Nuclear Security Administration under contract DE-NA0003525.

The authors would like to thank the following people for reviewing this report, Erik Marstein (IFE) and Marc Köntges (ISFH).

LIST OF ABBREVIATIONS

AC	Alternating current
ASI	All sky imager
BOS	Balance of system
CMSAF	The Satellite Application Facility on Climate Monitoring
DC	Direct current
ERA5	ECMWF Reanalysis Version 5
FM	Financial model
GCR	Ground coverage ratio
GHI	Global horizontal irradiance
GPU	Graphical processor unit
GUM	Guide to the expression of Uncertainty in Measurement
KPI	Key Performance Indicator
LCOE	Levelized cost of electricity
MERRA	Modern-Era Retrospective analysis for Research and Applications, Version 2
MODIS	Moderate resolution imaging spectroradiometer
MPPT	Maximum power point tracking
NCU	Network control unit
NSRDB	National solar radiation data base
PAC	Provisional acceptance certificate
PAR	Photosynthetically active radiation
PERC	Passivated emitter rear contact
PERT	Passivated emitter rear totally diffused
POA	Front side plane-of-array
PV	Photovoltaics
RPOA	Rear side plane-of-array
SAT	Single-axis tracker
SHJ	Silicon heterojunction
TCU	Tracker control unit
TMOD	Module temperature
VF	View factor

EXECUTIVE SUMMARY

Bifacial photovoltaic (PV) tracking systems, where bifacial PV modules are mounted to moveable racks that rotate the modules to follow the Sun, are the main utility-scale PV system configuration being currently deployed across the world. Today, over 90% of modules sold use bifacial cells and over 60% of the market share of systems installed use single-axis trackers [1]. The popularity of such system designs can be traced to the financial benefits of such systems. Typical tracker gains of 15-20% and bifacial gains of 2-10% are additive and these systems provide the lowest levelized cost of electricity in about 90% of the world [2].

This report provides an overview of current best practices to optimize the performance of such systems. The authors are international experts on these topics and have reviewed recent literature and industry standards for this report. In addition, 16 tracker companies (>87% of global market share from 2012-2021) and owners/operators of more than 13 GW of PV systems around the world were surveyed to learn about real world experience. Additionally, a blind modeling round robin exercise was run to evaluate the state of the art in simulating bifacial tracking system performance.

The different types of single-axis trackers and their components and features, including figures showing the complexity and variety of designs are outlined and design principles for matching the system layout to the site are presented. Several different tracking algorithms have been developed to increase energy yield per land area, including backtracking, which avoids row-to-row shading. Tracker companies are innovating to make their solutions applicable to a wide range of site conditions, including sloping topography. Recent innovations in tracking have focused on active protection of modules from wind, hail, snow and even flooding. By integrating with local sensors and weather forecasts, the trackers move to safer positions during these events. Tracker companies are also experimenting with novel ways to collect more energy during cloudy conditions with diffuse stow strategies, and also new backtracking methods that are customized for different module technologies (e.g., thin film, half-cell modules). Recent research has focused on developing backtracking strategies for complex terrains to minimize row-to-row shading and maximize light collection.

The practice of albedo enhancement using reflective engineered materials is reviewed. An important factor is the durability of these materials; many have been shown to not last for more than a few years or less. Current studies have shown that strategic placement of these materials can increase yields while minimizing material usage, but long-term durability will need to be demonstrated for albedo enhancement to be commercially viable.

Agrivoltaic systems (PV along with agricultural crops or livestock) offer an interesting application for bifacial tracking systems due to their ability to control the array tilt and adjust light reaching the ground. These systems also allow the farmers to move the trackers to accommodate farm equipment and activities. Increasing the height of the system leads to potential cost increases due to increased wind loads and stronger foundations. Several studies have shown that agricultural yields beneath the array can increase for some crops in some climates but decrease for many other crops.

Best practices for monitoring the performance of bifacial tracked systems is reviewed. Guidelines for measuring front and rear plane-of-array irradiance are discussed, including the required number of sensors and sensor placement to accurately measure these quantities. Recommendations for measuring back-of-module temperatures, wind speed and direction within the array, tracking angle (inclination), and surface albedo under the array are also given.

Three types of performance models used to simulate bifacial PV performance: view factor, raytracing, and GPU based 3D view factors are summarized and compared including selected commercial and open-source software that implement these methods. Finally, the results of a blind modeling comparison in which nine experts were asked to simulate six hypothetical bifacial PV tracked system designs using the same site and weather data are presented. This comparison demonstrated that simulation models do not yet agree, especially regarding rear side irradiance, module temperature, and tracking angles. More work is needed to generate high quality validation datasets for model developers to improve their models.

Tracker reliability considerations and failures are divided into intrinsic and extrinsic causes. Such failures can result in catastrophic system failures that damage other parts of the system (e.g., module damage from torsional galloping due to excessive wind loads and design flaws). Simulations of annual energy losses are presented for different scenarios where failures only result in tracker stalling.

Finally, topics related to the technical and financial optimization of bifacial tracking systems from the perspective of a project developer or investor are discussed. The LCOE metric, which is useful for comparing different sites and technologies is defined. Once a site and design are chosen, the yield assessment allows estimation of revenue streams throughout the project lifetime. CAPEX and OPEX are very important parameters for evaluating project viability and care should be taken to reduce uncertainty in these values by obtaining reliable quotes from local suppliers. Optimization of a project involves generating scenarios that vary technical and financial inputs to calculate internal rate of return for the project considering uncertainties.

The details in this report are intended to help companies and developers of PV projects to design and build PV systems that consider all the factors that might influence the future performance of the system and result in higher quality systems.

Key areas where improvements are needed include:

- **Tracking algorithms**: Tracking companies avoid sharing details about how their specialized tracking algorithms work and therefore it is difficult to evaluate their performance and assess whether they add sufficient value to the bifacial technology or to a particular project. Developers interested in new tracking algorithms are encouraged to deploy multiple sets of trackers each running different algorithms at a site for a test period to help decide which one to use for the life of the plant. Side-by-side comparisons at the same site are necessary to validate industry claims of potential yield increases.
- **Albedo enhancement**: It is not yet clear whether the use of albedo enhancers, such as geosynthetics, will ever be economically feasible, but early studies have shown some promising results. Continuing research into low-cost, durable materials and optimal placement strategies will help determine if albedo enhancement becomes standard practice.

- **Response to extreme weather**: The ability of trackers to respond to rare, extreme weather conditions should be standardized. According to our owner/operator survey, there is a significant risk that a tracker will not respond appropriately to such an event. While these events are rare, their consequences are very impactful.
- **Capacity tests**: While the standardization of monitoring for bifacial tracked PV systems has improved significantly in recent years, there are still serious challenges for completing capacity tests on these systems due to factors such as high dc/ac ratios, periods of cloudy weather, and uncertainty in row-to-row shading and yield predictions.
- **PV performance models**: Yield prediction (performance) models for bifacial tracked systems need to be improved. Our round robin model comparison carried out on six scenarios demonstrated up to ~100% difference between rear side irradiance predictions between different models and participants. Also, predictions for module temperatures and even tracking angles were alarmingly variable between different participants. More high-quality, validated datasets are needed for model developers to ensure that models are more consistent.
- **Reliability**: There is very little literature on the reliability and durability of single-axis tracker systems. Longitudinal studies of different tracker technologies across different climates need to be supported. Such studies are important for optimizing the design and operation of tracked PV plants.

The use of bifacial modules and trackers for agrivoltaic systems is especially exciting because if it can be shown to be feasible, it could make available a vast amount of land for renewable energy generation and help many smaller countries benefit from PV energy without sacrificing land for agriculture. A major challenge will be how to reduce the design complexity and variations for such applications to take advantage of standardization, high throughput manufacturing, and global supply chains to lower the cost.

1 INTRODUCTION

Bifacial photovoltaic (PV) tracking systems, consisting of bifacial PV modules mounted to moveable racks that rotate the modules from east to west following the sun, are the main utility-scale PV system configuration being deployed across the world. Today, over 90% of modules sold use bifacial cells and over 60% of the market share of systems installed use single-axis trackers [1].

The reason this pairing of new technologies has dominated the market for utility-scale PV is made clear by a 2020 technoeconomic study [2] that found that this system configuration resulted in the lowest levelized cost of electricity (LCOE) for 94% of the global land area. On average, bifacial, single-axis tracked systems had 16% lower LCOE and up to 35% higher energy yield than fixed-tilt monofacial PV systems. Figure 1 shows the difference in simulated yield between single-axis tracking (SAT) and monofacial latitude-tilt systems across the United States. SAT systems increase annual yields (**tracking gain**) by 15-20% (left) while adding bifacial modules to the comparison results in an additional 2-10% absolute increase (**bifacial gain**). Furthermore, **bifacial gain** and **tracker gain** are additive [3]. The largest relative increases appear to occur in regions with significant snowfall. While these dramatic performance predictions help to explain why this technology has been widely adopted by industry, the story of this technology pairing is more complicated when viewed at the site and project level, where many complexities can affect performance, reliability, and overall project success. This report aims to dig deeper into this subject and provide clear technical descriptions of the technology along with best practices and recommendations for developers, utilities, equipment manufacturers, and customers.

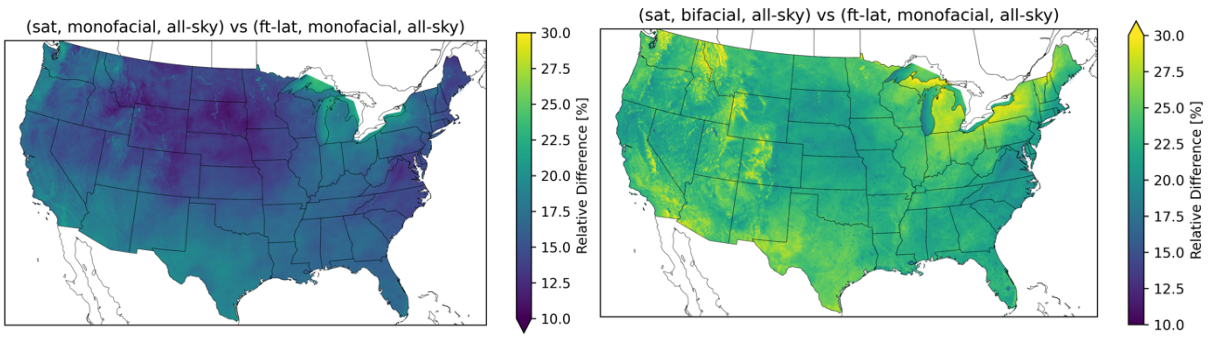

Figure 1 – Relative difference in annual yield for single-axis tracked monofacial (left) and bifacial (right) each compared with fixed-tilt monofacial systems predicted using pvlib-python (v0.10.5) and a GCR of 0.4.

1.1 Bifacial photovoltaic technology

Bifacial photovoltaic cells, modules, and systems have rapidly overtaken the market share of PV technologies. The 2024 ITRPV [1] estimates 90% of cells made in 2023 were bifacial and about 95% of modules used bifacial cells, with 62% made as bifacial modules and the rest as monofacial modules. Using bifacial cells in a monofacial module employing a white reflective backsheet increases module efficiency over using an equivalent monofacial cell. The fraction of bifacial modules is expected to reach 73% by 2034 [1]. Such rapid growth was enabled due to the advancement of PERC cell design that replaced opaque, monolithic back surface foil contacts with

isolated contacts, allowing light to reach the cell from the rear side. Minor improvements to cell processing steps have resulted in bifacial solar cells with rear side efficiencies of PERC cells around 70% of the front side (**bifaciality factor**). Bifacial cells now come in many varieties (e.g., PERC+, n-PERT, SHJ, n-TopCon etc.) with bifaciality factors approaching 90% for some SHJ cells, and most cell lines have converted to producing bifacial cells. PERC+ cells with a bifaciality factor of 70% are currently the most common in the market. TopCon cells have bifaciality factors of 80%. More details about this PV technology transition are available elsewhere [4-6]. This report focuses on bifacial PV modules, not on monofacial modules with bifacial cells.

1.2 Market surveys

In order to better understand the diversity of PV trackers offered in the marketplace and to learn about plant owner and operator experiences with these systems, two surveys were conducted.

Tracker manufacturer survey: 16 tracker companies that represent >87% of global market share from 2012-2021 were surveyed. Questions focused on the company history and position, product features and specifications, tracking algorithms, and environmental, social and governance stance. Figure 2 shows where companies are headquartered and the types of trackers that they sell. Horizontal SATs are the most popular. Other types of trackers include 2-axis trackers and tilted single axis trackers (TSAT), where the torque tubes are tilted toward the equator.

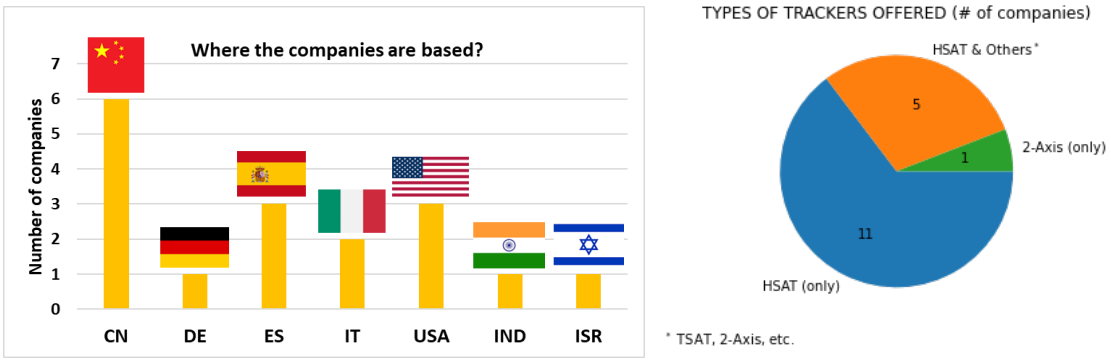

Figure 2 – Headquarter countries for tracker companies surveyed (left). Types of trackers offered (right).

Tracker owner/operator survey: Owners and operators representing 13.4 GW of systems around the world were surveyed. Figure 3 illustrates the distribution of the professional roles of the survey respondents. The primary objective of the survey was to understand users' preferred technical specifications, most utilized configurations, experiences faced during extreme events, and perceptions of tracker system reliability.

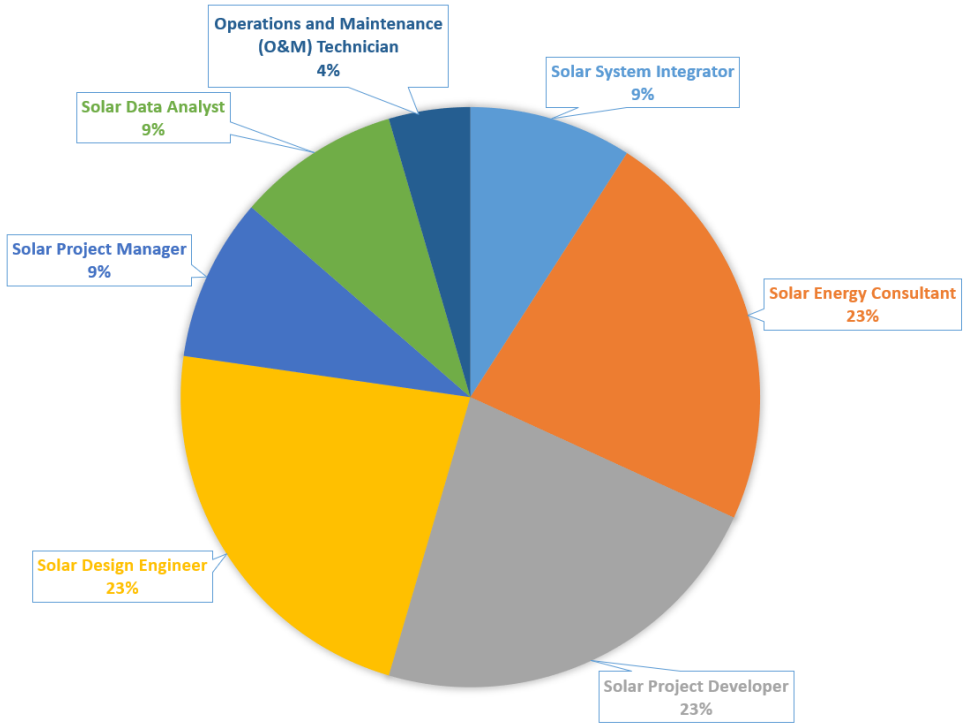

Figure 3 – Professional categories of owner/operator survey participants.

Although the single-axis tracker concept is more than 30 years old [7], the tracker industry is quite young and very international. All but one of the participants in the tracker manufacturer survey have been in business less than 20 years. 50% sell trackers in >20 countries and >80% sell in more than 10 countries.

Among the participants of the tracker owner/operator survey, 82% indicated their use of single-axis solar trackers in combination with bifacial module technology, highlighting a trend towards the adoption of PV systems integrating both these technologies. When asked to rank their reasons for choosing SATs from 1 to 5 (with 5 being the most important), the top choice was the reduction of LCOE with higher energy gains and tracking and backtracking strategies coming in second. In addition, users also valued features such as self-powered trackers, connectivity with user-friendly software, strategies to handle extreme weather conditions, and adaptability to different foundation types and terrains. Figure 4 shows the average ranking of all responses for each feature/factor.

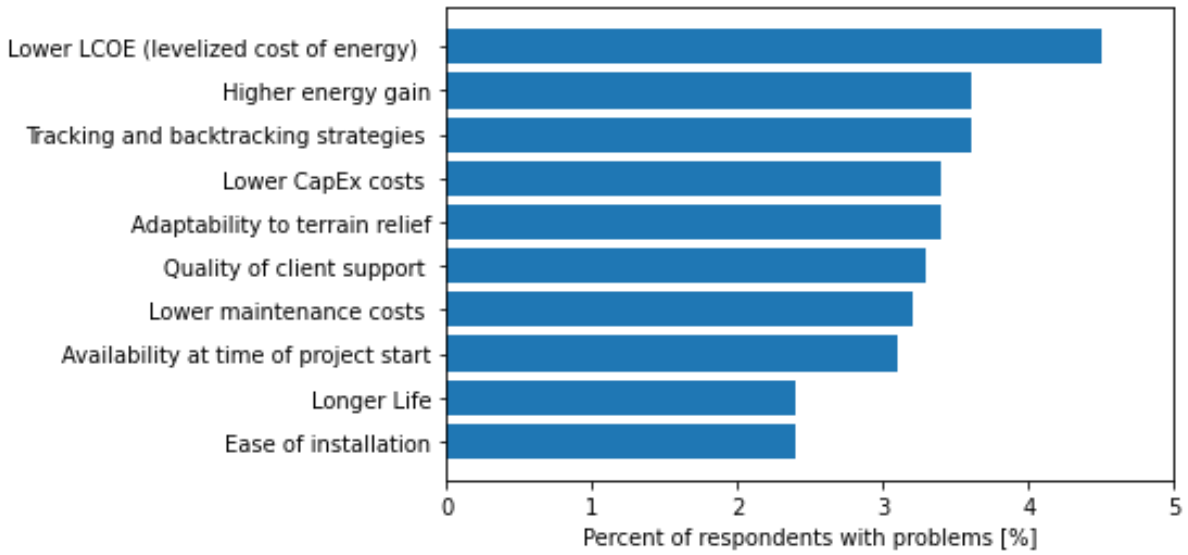

Figure 4 – Key features/factors influencing tracker selection according to surveyed users. Values are average ranking of all responses.

The main tracker configurations identified by owner/operators are 1P, 2P, and in some cases 2H. While 2P used to be popular, 1P is largely favored now due to it being easier to install and lower wind loading requirements. The 2P configuration is favored for agrivoltaic configurations largely due to the greater hub height and pitch, which allows agricultural activities under and between rows.

The popularity of the SAT design is attributed to the significant tracker gain and yield per area (efficient use of land) compared with fixed tilt systems. Design improvements and efficient supply chains have kept tracker costs low and reliability high, which has resulted in the lowest system LCOE for many utility-scale applications. Depending on the site's latitude and layout (ground coverage ratio, topography, etc.), SATs will have tracker gains between 15-20% more energy annually than an equator-facing fixed-tilt system with equivalent capacity [3, 8, 9].

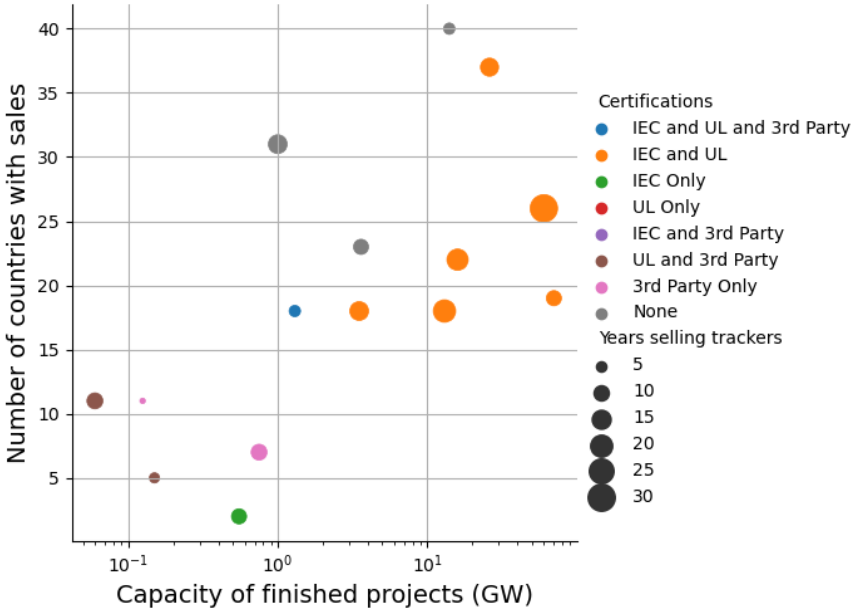

Figure 5 – Summary of number of countries in which tracker manufacturers sell their products, number of years in the market and certifications offered on their products. 'IEC' indicates certification to IEC 62817, 'UL' indicates certification to UL 2703 [10] and/or UL 3703 [11], and '3rd Party' indicates third party engineering reviews and/or bankability studies (not including wind tunnel tests).

Figure 5 shows the correlation between the number of countries that participating tracker companies reported sales in versus the total GW capacity of their completed projects. The smallest company interviewed completed 0.75 GW of projects and the largest company completed over 70 GW. One company did not answer this question. The size of the markers in Figure 5 corresponds to how long each company has been selling trackers (2-31 years). The marker color categorizes how companies responded to the question 'Do your trackers have any certifications?'. All companies that hold UL 3703 [11] and IEC 62817 [12] certifications for trackers have completed more than 1 GW of projects and have been in business for at least 6 years. Our results indicate that younger companies and companies with total projects less than 1 GW tend to demonstrate their bankability with third party certificates from organizations such as Black & Veatch, DNV, or VDE.

2 SYSTEM DESIGNS FOR OPTIMAL YIELD AND VALUE

2.1 SAT Tracker Types and Operational Modes

Most models of horizontal SATs share many common components and features [13]. Most trackers have **torque tubes** attached to **bearings** and **motors**, which are mounted onto **posts**/**piles** that are attached to a solid **foundation**, which securely connects the structure the ground to prevent. movement. The depth, strength, and materials of the foundation are customized to the site based on geotechnical conditions, soil type, maximum predicted wind speed and wind loading calculations. **Purlins**/**rails**/**omegas** are attached to the torque tube for the purpose of mounting modules using **clips** or bolts. SAT configurations are described by the number of modules mounted perpendicular to the torque tube and the module orientation. For example, a **1Up Portrait** or ***1P*** system has one row of modules mounted in portrait along the torque tube. For bifacial systems, portrait orientations (1P, 2P, etc.) are preferred since modules are designed to be mounted along their long edges. In contrast, landscape orientations (2L, 4L, or 6L) require two purlins to cross the back of each module to attach them along their long edges. Having purlins cross the back of bifacial modules can reduce the rear side irradiance and result in less bifacial gain.

Figure 7 captures some of the key mechanical and electrical specifications from 13 tracker companies that responded to these questions. Figure 7 shows that most companies offer trackers that can be installed on a 15% (8.5°) maximum overall north-south grade. Companies were not asked to report their tracker articulation limits (i.e., the maximum torque tube slope change between piles or piers). The slope tolerances for the east-west grade tend to be greater than north-south with three companies reporting that their trackers have no slope limitations in the east-west direction. Figure 7 also shows that the maximum row length is negatively correlated with the maximum overall north-south slope. For instance, the company that reported the highest maximum north-south slope of 30% (16.7°) also reported the shortest row length of 25 m.

The marker shapes of Figure 7 show the options that companies offer to power their trackers (motor and electronics). The companies fell into three categories offering either AC grid powered, PV powered with batteries, or they offer both options to customers. ‘PV-powered’ here either refers to the use of a single dedicated PV module, or a parasitic load from a sub-string of PV modules. The survey did not ask companies about their battery backup options. Only one company uses AC motors exclusively; all other companies use DC motors. The colors of Figure 7 show how many rows can be moved with one motor wherein 15 responses stated 1 or 2 trackers can be rotated with a single DC motor, and one outlier stated that 32 trackers can be moved with a single AC motor.

Tracker manufacturer survey results for the maximum tracker tilt angle were more consistent with 14 responses of either 55° or 60°. One company reported a maximum angle of 52° and one did not respond. Some companies noted that these limits were imposed via software to provide a safety margin to the gearbox’s hard limit. In this regard, two companies reported a max angle of 90°, but the 90° angle was only intended to be used during special activities like harvesting of agriculture (tracking limits were still ±55° or ±60° in continuous operation).

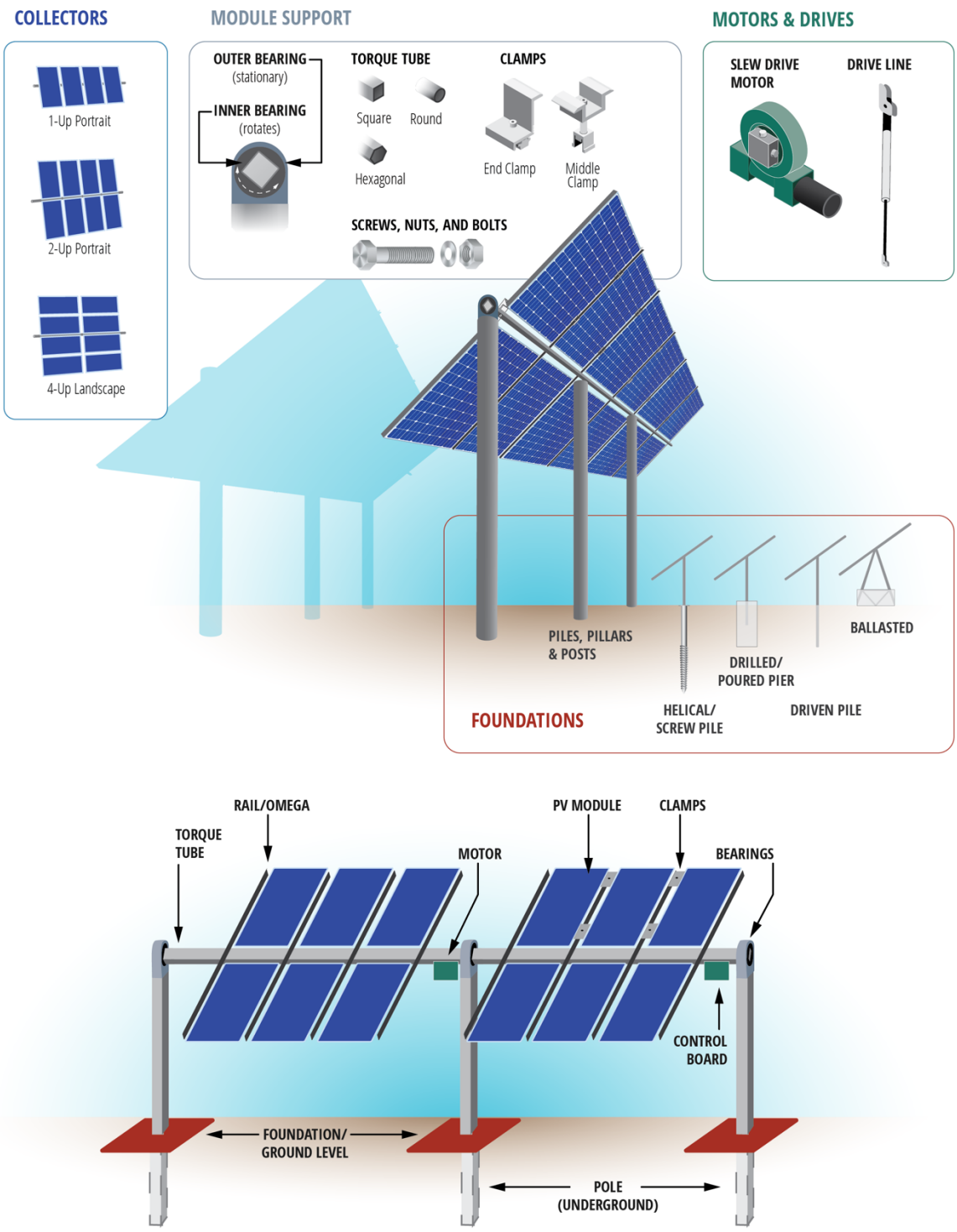

Figure 6 – Bifacial tracker system design features and relationships with bifacial performance. From left to right in the diagram the level of detail increases.

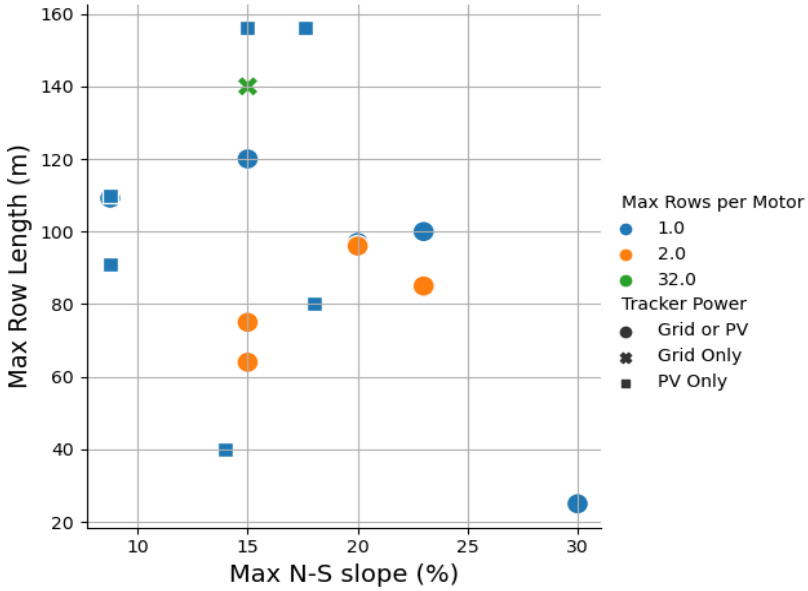

Figure 7 – Tracker maximum row length versus maximum installation slope and tracker power options.

2.2 System Layouts

SATs maximize the output of PV-generated energy by changing the array tilt angle to minimize the angle of incidence between the Sun and the array and the vector normal to the array. SATs, despite being more expensive to build and maintain than fixed-tilt arrays, can lower the LCOE due to the extra energy produced. To realize this extra energy the site characteristics, including latitude must be considered.

Designing the layout for a PV system with solar trackers involves several considerations, including the type of solar tracker, the terrain, available space, shading tolerance, and the orientation of solar modules for maximum sunlight harvesting throughout the day. The key elements for designing a PV system tracker layout include:

- **Site Assessment.** Due to the combination of low PV module prices and high land costs, optimizing the arrangement of PV modules on land is essential for maximizing the return on land investment [14]. In this context, the design goal is usually to maximize energy production per unit of land area rather than maximizing energy production relative to the peak DC power rating [15]. Site assessment considers factors such as available land area, solar resource and weather/climate, topography, and albedo. In addition, geotechnical assessments of soil structure and properties are important for selecting foundation and support structure materials and evaluating corrosion risks. Seismic and flooding risk evaluation is also done during site assessment. Several studies have indicated that the design complexity of PV systems increases as a result of complex topography [16]. PV installations over water are not considered in this in this report.
- **Solar Tracker Type.** Site assessment plays a critical role in determining the appropriate tracker type and row length, considering specific topographic variations. Options range from independent-row architectures, where each row

operates autonomously, to dual- or multi-row systems with shared actuation. The choice between these types is informed by land topography and may also impact tracker row length. During the design phase, careful consideration is given to the configuration of the structural rails and supports on the tracker and how it may lead to **structural shading**, where material on the tracker blocks light from reaching the rear side of the bifacial modules. This step is essential for avoiding losses to bifacial gain. Commonly, single-axis trackers employ a 1-Up Portrait Configuration, with modules positioned parallel to the East-West direction. However, this setup places the torque tube directly beneath the modules' midpoint, which can be suboptimal for maximizing rear side irradiance gain for certain modules. However, recent module designs that place junction boxes along the centerline of the module are ideally suited for 1P designs. Alternatively, a 2-Up configuration places the torque tube between the two modules and minimizes structural shading on the rear side of the bifacial modules. The tracker structure can minimize shading for specific configurations by adjusting gaps between modules along the torque tube to further enhance rear side irradiance gain [17], the height of the torque tube, and the spacing between contiguous modules. To minimize mismatch between upper and lower rows, separate Maximum Power Point Tracking (MPPT) systems are generally employed for each horizontal string [18].

- **Spacing and Orientation.** SAT rows are typically aligned with a north–south axis, varying the tilt of the arrays from east, in the morning, to west, in the afternoon. The spacing between trackers' rows is called **pitch** and is determined by defining a **Ground coverage ratio** (GCR), which is equal to the total module area divided by the total land area for the system. Pitch is inversely proportional to GCR. Higher GCR values may increase energy production potential per land area by allowing more PV to be installed for a given area, however higher GCR systems suffer from increased periods of row-to-row shading, reducing overall efficiency. **Row-to-row shading** also called **self-shading** can be minimized with backtracking but result in periods of non-optimal tracking angles and lost energy.

Considering all these factors during the design of large PV plants can be challenging and design decisions will differ depending on the specific site characteristics. Modeling software such as PV CASE, PVsyst, and SAM already facilitate the design and layout optimization of PV SAT systems and incorporate models to account for bifacial modules. A recent study [16] proposes a generalized algorithm to optimize the placement of SATs considering topography. The algorithm implemented in Mathematically™ software begins by designing inter-row spacing to prevent shading between modules and uses geospatial data from satellite images via QGIS software, identifying available land areas for PV module installation. Despite the complexity posed by irregular land shapes, the study calculates the effective annual energy incident on PV modules. It considers and compares 1P and 2P mounting configurations allowing designers to optimize system designs.

2.3 Extreme weather response

Tracker systems utilize various strategies to protect the structure and PV array from extreme weather events such as high winds, snow, hail, and floods. PV tracker systems typically respond to high wind speed by moving solar modules into a **stow position** to reduce static and dynamic wind loads and to reduce the likelihood of resonant vibrations and torsional galloping [19, 20]. Anemometers and wind direction vanes are used to monitor for high wind speeds. However, the wind stow thresholds and stow angles vary among tracker designs and suppliers. For example, responses from the tracker company survey showed wind stow thresholds were 15–22 m/s, and the stow positions varied from horizontal to 5–30° tilt toward the prevailing wind direction. Some companies mentioned that their trackers use different stow strategies for gale force and hurricane level winds ("survival mode"). Finally, some companies noted that trackers located near the perimeter of a PV plant could be set to have a different stow strategy than trackers within the plant to respond to differing local conditions.

In some cases, tracker control systems automatically detect hail and adjust modules to a steep inclination that minimizes impact energy. Advanced tracker control systems may also include flood sensors that orient the array into a horizontal position when triggered. These advanced features are typically add-ons to companies' standard product offerings. A common feature in most trackers is a manual override for operators to control module positioning in anticipation of bad weather or for O&M activities.

An active area of development is the connection of remote monitoring and automated control systems to adapt to changing weather patterns and short-term forecast data. Nowcasting techniques can achieve high resolution forecasts for the near future. Usually these are achieved through a combination of irradiance measurements and fisheye sky cameras installed on the ground, namely all sky imagers (ASIs). Recent developments in this field involve the creation of a hybrid model. The integration of machine learning for irradiance retrieved from ASI based models and satellite based nowcasts, provides higher-resolution weather predictions that allow system operators to respond to extreme weather and avoid catastrophic damage [21]. In addition, longer-term weather forecasts are used to anticipate extreme weather risks and prepare plants by stowing trackers prior to storms or to ensure staff are onsite to respond to events.

The renewable energy insurance company GCube released a report stating that only 1.4% of their PV insurance claims in the last five years were for hail-related damage, but that this small number of claims amounted to 54% of their total incurred costs [22]. In other words, catastrophic hail damage is rare, but it is incredibly costly when it happens. The report mentions that hail damage was exacerbated by trackers either not stowing or not stowing correctly.

The tracker manufacturer survey asked tracker companies if and how their trackers respond to hailstorms. Figure 8 **Error! Reference source not found.**shows that 11 companies claim to have either an automated or manual response to hail events. Only 2 companies mentioned that their trackers have no hail strategy implemented, and 3 companies did not answer the question.

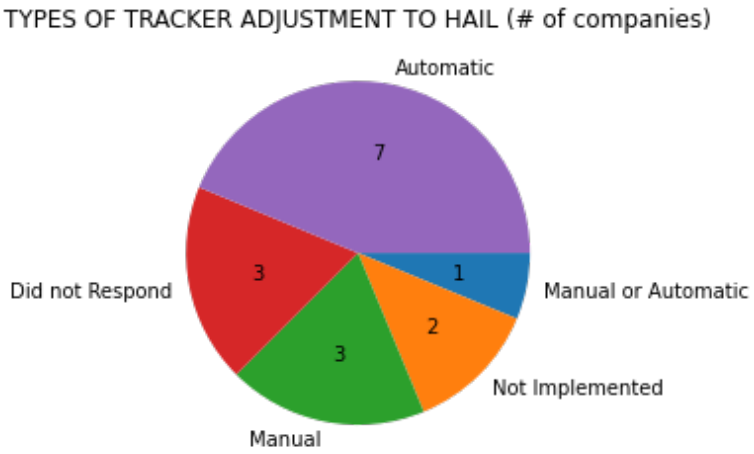

Figure 8 – Pie chart showing answers from 16 tracker companies to the question 'Describe how your trackers adjust to hailstorms'. 11 out of the 16 companies claim they have either an automated or manual hail response strategy.

Table 1 illustrates responses from the owner/operator survey regarding the readiness of their trackers for the specific extreme events. The percentages represent the proportion of users who answered affirmatively to the event.

Table 1 – Owner/operator survey responses on how trackers respond to extreme weather events.

	Hail	Flood	Snow	Wind
Yes	30%	45%	70%	100%
How	Weather forecast	On site sensor	On site sensor	On site sensor
What	Rotates to maximum tilt wind stow strategy dominates	Moves to flat stow position	Moves to full tilt position	Moves to flat stow position

The effective trackers' responses to extreme weather events varied significantly according to user feedback. Approximately 50% of user responses indicated that they had had experience with trackers and/or modules being damaged due to inadequate tracker response to extreme weather conditions. Conversely, around 45% of respondents reported that the trackers performed as expected according to the manufacturer's documentation. A small percentage of respondents did not provide specific feedback in this regard. Overall, the majority (65%) of respondents reported experiencing damage from extreme weather events, highlighting the importance of robust designs and weather response mechanisms in tracker systems. Several reasons for inadequate tracker responses were identified. These include instances where the tracker response was not triggered properly, incorrect wind stow parameters were set, or the extreme weather event surpassed the manufacturer's specifications. Weak points contributing to damage were challenging to pinpoint to a single component, but

generally included modules, trackers, bolts, clamps, and balance-of-system (BOS) management. Loss of communication between components also emerged as a significant issue exacerbating damage and hindering timely responses during extreme weather events.

2.4 Tracking algorithms and controls

Based on the type of control strategy, the solar tracking technology can be divided into **open-loop** and **closed-loop** systems [13, 23, 24]. Algorithms with open-loop control do not require any sensors to detect the sun position. The sun's path is calculated by a local microprocessor, which, based on programmed geographic position and astronomical relationships, calculates the sun's position at any time of the day throughout the year. Some manufacturers integrate GPS devices to enhance accuracy by gathering latitude, longitude, date, and time data. These algorithms ensure continuous tracking regardless of irradiance conditions, except during high winds when trackers stow for safety. Open-loop controls are particularly beneficial on partly cloudy days or during variable irradiance conditions, because the tracker remains in position to take advantage of short sunny periods without delays for repositioning [25].

In contrast, closed-loop control algorithms use irradiance sensors or inverter output to adjust tracker position. Sensor data guides a control unit, activating motors and actuators for precise tracking. However, optical sensors may require calibration [26] and can be influenced by reflected light from surrounding obstacles [27]. In adverse weather, such as cloudy skies, trackers may expend additional energy searching for the optimal position due to light dispersion.

To obtain more accurate tracking, the open-loop and closed-loop strategies can be combined as the **hybrid-loop** system, including a coarse control implemented in open-loop and a fine control performed in closed-loop [28].

SAT Tracking algorithms

SAT trackers typically offer at least two tracker algorithms designed for different module types. **True-tracking** [29] rotates all rows to minimize the incidence angle between the Sun and the normal vector to the front side plane of the array (POA) (Figure 9). True-tracking results in row-to-row shading early and late in the day but is a preferred algorithm for CdTe modules because of their linear shade response [30]. **Backtracking** is the same as true-tracking in the middle of the day, but it adjusts the tracking angle of all rows towards horizontal in the morning and evening to prevent row-to-row shading (Figure 9). By 2020, many commercial single-axis trackers adopted backtracking methods similar to that proposed in 2011 [31], although the backtracking concept dates back to the early 1990s [7]. This geometry assumes a horizontal tracker placement, eliminating vertical offset considerations between rows. Further work introduced the concept of **slope-aware backtracking** [32, 33] which extends the backtracking algorithm to consider axis tilt and cross-slope topography (Figure 10). It introduces the shaded fraction of module area for trackers on a cross-axis slope at any rotation, but its applicability is limited to sites with mono-sloping (non-undulating) terrain. Anderson and Jensen recently extended the slope-aware backtracking model [32] to apply to rolling 2D terrain [34]. The shaded fraction equations provided in [34] permit study of **partial-tracking** strategies in complex 2D terrain. Presently, the authors

are not aware of analytical methods for deriving the shaded fraction of trackers in 3D terrain, likely due to the complexity of the solution. However, non-analytical methods such as ray-casting have been proposed as a means of calculating optimized backtracking angles in complex 3D sites [35]. One challenge with applying such calculations to as-built systems is the common minor discrepancy between system drawings and the real system. At low Sun angles such small differences can result in unanticipated row-to-row shading.

A brute-force approach to minimizing interrow shade losses in tracker sites with complex topography is the so-called **GCR-adjusted tracking** method [36]. In this approach, the GCR input parameter used in the backtracking algorithm is manually and gradually increased until shading losses decrease to an acceptable level. For c-Si modules that use bypass diodes, any shading can result in a disproportionate loss of power, thus backtracking is generally preferred, although the diode-placement inside of the modules with half-cut cells enables so-called **half-tracking** or **partial-tracking** algorithms [34, 37, 38]. Dobos [38] reported long-term energy gains of 0.7%–1.5% over standard backtracking when a proprietary partial-tracking strategy was employed. In general, more research is needed to quantify the benefits of the partial-tracking approach and under which conditions it should be applied. A technoeconomic analysis of backtracking strategies showed that standard backtracking was able to reduce LCOE by up to 9% and advanced strategies that calculate irradiance at all tilt angles to achieve a global optimum could achieve up to 12% reduction in LCOE [37].

Tracker algorithms can also have complex responses to different situations. **Diffuse-response** algorithms [39-41] orient the modules to horizontal when skies are cloudy to capture more diffuse light. However, other studies have proposed a new approach, called the **Analytical algorithm** [42]. This is based on the fact that, depending on the radiation conditions (fraction of beam and diffuse of the global radiation), the optimal angle may be an intermediate position between the horizontal plane and the angle set by the True-Tracking algorithm. Moreover, on days with cloudy intervals, an intermediate position makes it possible to be closer to the optimum position in the event of a clear or cloudy day, reducing the number of turns and the consumption of the drive. **Self-cleaning** algorithms [43] tilt the modules during precipitation events or when conditions will lead to dew formation to allow water to flow easily off the modules and wash away dirt or snow. **Hail-response** and **wind-response** algorithms [19] place the rows in orientations to protect the modules from damage (e.g., tortional galloping). While most true-tracking and backtracking algorithms use open-loop controls that follow an astronomical Sun position derived from the time, latitude, longitude, and well-known movement of the Sun, diffuse-response, self-cleaning, hail-response, and wind-response algorithms require closed-loop controls and knowledge of environmental variables from internal sensors or external signals such as weather forecasts. If hail risk is high, consideration of maximum rotation speed may be important, especially if there is not much warning of impending extreme wind or hail. Soltec reports a tracker rotation speed of 20° per minute [44], Nextracker reports up to 40° per minute [45] and other trackers have slower speeds, which means some may take several minutes to move to a stow position in response to wind or hail. Some algorithms require human intervention. 15 of the 16 tracker companies interviewed reported a wind-response strategy. In Section 1.3 (Extreme Weather Response), the wind speed threshold and stow angle parameter settings that are commonly used by

the surveyed companies are summarized. The companies did not mention if owners/users can modify these parameter settings, which are determined by the structural design, location, probability for extreme-weather, as well as insurance and risk-aversion plan established by the owners and system managers. Interestingly, there does not appear to be any tracking algorithms specifically designed for enhanced albedo conditions.

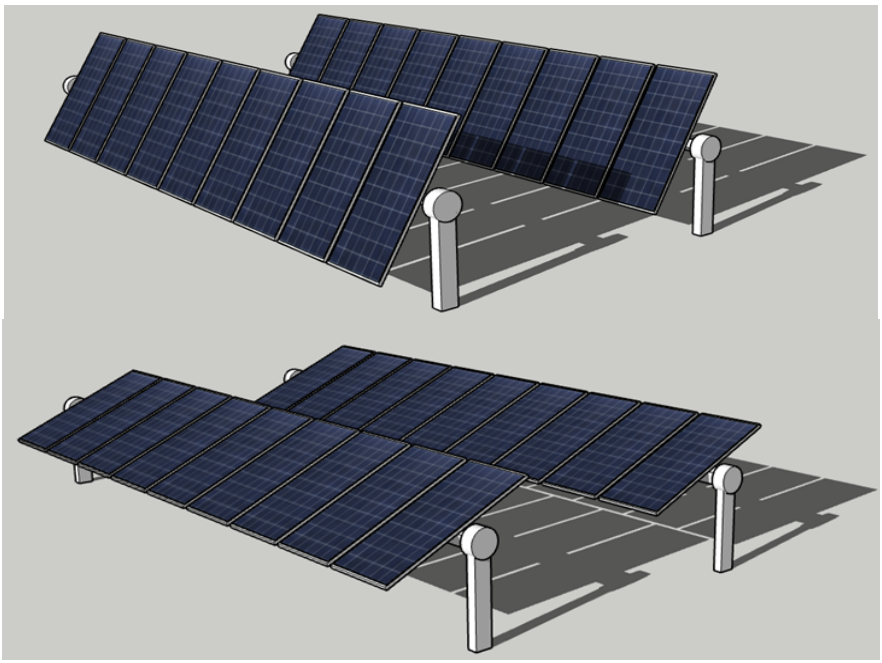

Figure 9 – True tracking (top) and backtracking (bottom) compared at low Sun angles. (image from Sandia).

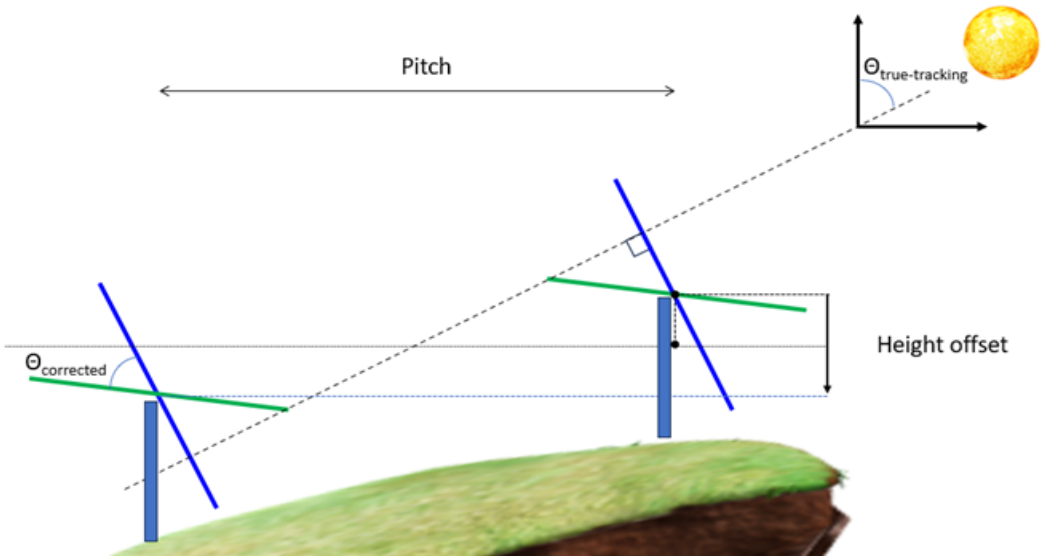

Figure 10 – Slope-aware backtracking compared with true-tracking.

2.5 Albedo optimization

Albedo is a measure of the reflectivity of a surface and is an important property to consider for the ground cover around bifacial PV plants. Depending on the kind of soil and vegetation, the **natural ground albedo** can range from 10% to 30% and may change seasonally. For reference, fresh snow has an albedo of 90% [46]. Light that falls on the ground between the tracker rows (mostly direct light) and below the bifacial modules (mostly diffuse light) is then partially reflected in every direction (isotropic reflection). Some of that reflected light falls back onto the rear side of the bifacial modules and is transformed into additional energy, referred to as bifacial gain.

Albedo optimization, also called **albedo enhancement**, refers to the practice of placing sheets or layers of high-albedo (white) material (albedo enhancers) on the ground to increase the reflected light. This leads to a further increase of the bifacial gain beyond the natural ground albedo. Such a practice may be warranted if the additional energy is worth more than the cost of applying and maintaining the albedo enhancer.

The most common form of **albedo enhancers** are white, reflective geosynthetics (examples shown in Figure 11), which are durable polymeric materials traditionally used in civil and environmental projects [47]. They include geotextiles, which are synthetic fabrics that allow water to infiltrate, and geomembranes, thin impermeable synthetic membranes used primarily for containment of hazardous substances. However, other materials such as sand, shells, salt and spray-coating of calcium-based mixtures have also been tested.

Figure 11 – Two examples for applications of albedo enhancers under bifacial trackers in large-scale PV power plants. Left: large-scale test of Solmax's Geolux albedo sheets (geomembranes) in Brazil (photo: Recurrent Energy), Right: Magnifield albedo enhancers (geotextiles) installed in a multi-MW power plant in Italy.

Typical albedo values of albedo enhancing materials range from 60-75%, roughly three times the amount of the normal ground and therefore, in theory, able to triple the bifacial gain. With bifacial gains for SAT typically ranging from 2-10%, this potentially means an additional bifacial gain of 4-20% absolute. However, considering the cost of the material and inverter clipping and/or curtailment of the powerplant, only half of this value may be realistically achieved.

To maximize the return-on-investment project owners must weigh the total cost of ownership against the lifetime benefit. With material prices around $1 – $2 USD/m² and current electricity prices, covering the entire ground is not likely to be economically feasible unless the added value, such as vegetation control, is shown to offset the extra costs. Other considerations are also important. For example, the geomembrane system used in Brazil and shown in Figure 11, requires biweekly mosquito control due to rainwater collecting on the surface and a risk of dengue fever in the area. Research investigating the **optimal placement** of the albedo enhancers [47-49] has found the positioning of the material directly below the modules is recommended. PV performance models (Section 4.1) can be used to simulate different spatial configurations of albedo enhancers and thus optimize designs. Figure 12 shows an example of using PVRADAR software to estimate the effect of albedo enhancers.

Figure 12 – Screenshot from PVRADAR software showing the effective and virtual bifacial gain (normal ground) and extra gain from optimally applied albedo enhancing materials.

Understanding irradiance increase in the tracker system is only the first step. Calculating yield and system **clipping losses** is also important to correctly quantify the economic value of albedo enhancers [48]. Inverter capacity may be sized only considering the nameplate (front side) production of the module. However, the bifaciality of the modules and the additional reflection from the albedo enhancers should be considered. The **effective gain** refers to the additional energy that is supplied at the grid connection, while the **virtual gain** refers to the additional energy that could have been produced if there had been no inverter limit, i.e. the difference being the energy lost by inverter clipping.

Interestingly, in cases when the inverter is a limiting factor, albedo enhancers become more effective over time due to module degradation. As the module efficiency decreases, albedo enhancers partially compensate for some of the lost capacity as virtual gains are converted to effective gains. (Figure 13). This underscores the

potential value of albedo enhancers, particularly in the context of repowering measures. A similar effect may be observed when switching from a fixed tariff to a time-of-use-tariff with higher sales prices in the morning and evening when clipping usually does not occur.

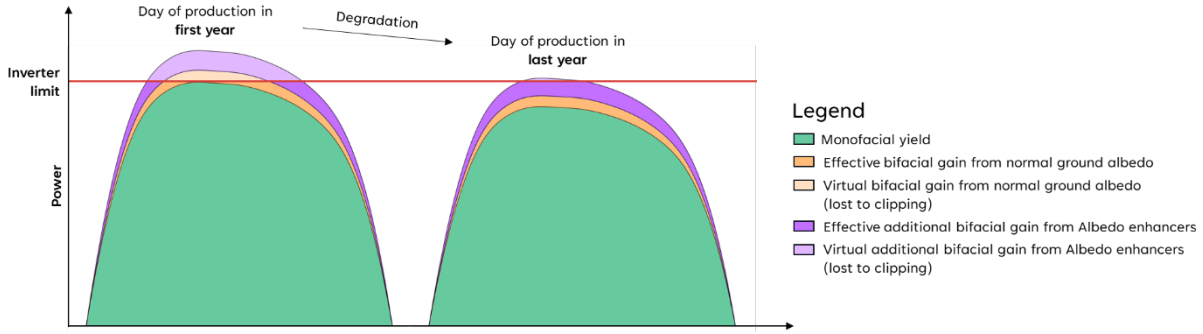

Figure 13 – The evolving impact of module degradation and albedo enhancers.

Albedo enhancers also present several **O&M and sustainability challenges.** While some materials can reduce O&M costs due to avoiding seasonal vegetation growth, the material itself can incur extra O&M costs for cleaning, maintenance, or reapplication.

- **Soiling & Cleaning**: Soiling can lower the cover's reflectivity, reducing energy gains (Figure 14). Typically, with bifacial gains at around 10% and assuming soiling rates of a similar magnitude, a rule of thumb suggests cleaning the cover about one-tenth (10%) as frequently as the front side of the modules. For example, if modules are cleaned annually, the albedo enhancer should be cleaned/refurbished roughly once every 10 years.
- **Degradation and damage**: Geosynthetics producers report stable high albedo values under prolonged UV exposure in lab tests. According to experiences in the field, the primary risk to material longevity stems from failures in the attachment to the ground, leading to tearing, wear, or wind-induced uplift and transport.
- **Safety**: For some materials, worker safety can also be a concern as it can add tripping and slipping hazards, as well as being an optical nuisance for O&M crews.
- **Sustainability**: Effects such as material composition, recyclability, and water run-off properties should also be considered. In addition, it is important to understand how the application of albedo enhancers might affect vegetation, animals, local runoff and other site-specific features.

Figure 14 – (left and center) - Commercial solution of spray coating albedo enhancer, 2 years on field [50]. (right) Soiling visible on a plastic-like material albedo enhancer. Photo Credits: NREL (left), Silvana Ovaitt (center-right).

The tracker manufacturer survey asked the question “Do you know of any client's projects that use or test albedo enhancers?” to which only one company replied ‘yes’. This particular ‘yes’ response was because the company’s split rail style foundation increased ground reflectivity relative to the natural ground. The sparse feedback from this survey question implies that tracker companies themselves do not commonly offer albedo enhancement as a product/service.

2.6 Agrivoltaic bifacial tracking applications

One of the most common dual uses of bifacial PV and trackers is for agrivoltaics. IEA PVPS 13 Subtask 2.2 is preparing a report on agrivoltaics, which will provide greater insights on the performance and reliability of agrivoltaic systems. Agrivoltaics refers to the dual use of land for both agricultural use and PV energy production. The definition and requirements for what constitutes an agrivoltaic system are not universally settled and can vary widely. For example, some frameworks place requirements on the PV structure’s minimum clearance height and maximum ground coverage [51], which may preclude tracker installations with standard dimensions and layouts from qualifying as agrivoltaic projects in certain countries. Meanwhile, other definitions do not place constraints on the PV structure used, but rather describe agrivoltaics as any dual use of solar-occupied land that provides ecological or agricultural benefits [52].

Trackers for agrivoltaic applications can expand the areas possible for PV installation, and often provide extra value for farmers, potential crop yield increases [53, 54], among other tangible benefits. It has also been a successful way for increasing clean energy acceptance in communities.

Our tracker manufacturer survey asked the question ‘Do you develop trackers for agrivoltaic applications?’ to which 11 out of 16 companies responded ‘Yes’. These 11 tracker companies reported a cumulative tracker sales volume of 19 GW in 2022 with average sales activities spread across 20 countries. Although the agrivoltaic capacity these companies deployed was not disclosed, their involvement in agrivoltaics demonstrates a considerable commercial potential and interest. Eleven of the same companies were asked to elaborate on the typical design modifications to their products that are used in agrivoltaic applications. Figure 15 shows the results with the values next to the bars showing the companies’ reported deployments in 2022. The modifications include combinations of: increased tracker height (N=8), wider row

spacing (N=4), modifications to the tracker algorithm (N=2), integration of agricultural sensors (N=2), and specialized hinging that allows the PV array to be oriented at 90° when agricultural tasks are performed (N=2). However, an opposing sustainability view was held by at least one company that chooses not to design trackers for agrivoltaic projects, but rather for only non-farmable, uneven land, so that farmland can be designated specifically for agricultural use.

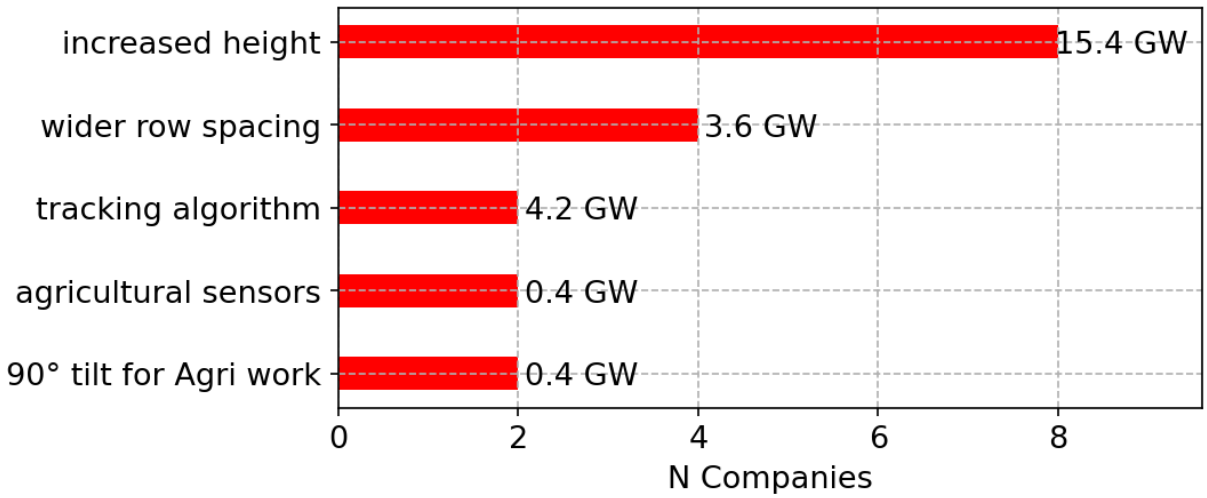

Figure 15 – Summary of the most common modifications reported by 11 tracker companies who indicated that they design trackers specifically for agrivoltaic projects. The value next to each bar shows the companies' total volume in 2022.

The versatile movement of solar trackers offer unique opportunities when used in agrivoltaic applications, which compared to traditional fixed tilt structures, may allow for expanded options for plants under the PV array [52]. For example, trackers can be oriented to a suitable position when agricultural work is performed between rows (Figure 16 **-** top left). The movement of trackers also allows control of the ground shade fraction received by crops through so-called '**anti-tracking**' [55] or 'controlled-tracking' techniques [56]. Wilcox et al. [55] field tested an approach wherein the PV array was moved off sun during periods when sunlight was most needed by crops. They demonstrated that compared to standard sun tracking, anti-tracking can significantly improve the homogeneity of photosynthetically active radiation (PAR) reaching the ground, but at the expense of PV energy yield. Valle et al. [56] tested a similar method on two lettuce varieties in France. Their modified algorithm oriented the PV array normal to the Sun for only four hours midday when irradiance is highest, but outside this window, the algorithm turned the PV array parallel to the sun beam. The modified tracking approach yielded biomass productivity similar to full sun conditions (i.e., with no PV), but only in the spring season, and with a substantial loss of PV energy.

Many agrivoltaic test sites are experimenting with different PV designs and technologies paired with a wide variety of crops. European Energy is testing different tracker positions for crop sewing activities in Denmark (Figure 16 – top left). Fraunhofer ISE is experimenting with elevated SATs to accommodate larger farm machinery [57] (Figure 16 – top right) and higher crops such as apples in Bavaria, Germany [58] (Figure 16 - center left). Jack's Solar Garden [59] (Figure 16 – center right and bottom left in Longmont, Colorado, U.S. is a 1-MW agrivoltaic plant with 8-ft tall trackers, which

facilitates tractor usage. Planting and much of the agricultural work otherwise is done by hand, which means good cable management practices behind the modules and between the rows is necessary to ensure the safety for agricultural workers. NREL has built an agrivoltaic test bed in Golden, CO, U.S. [60] (Figure 16 – bottom right). Early results appear to indicate greater agricultural yields from crops under the trackers compared with the controls.

Figure 16 – (top left): Custom 2P tracker angle positioning during interrow crop sowing in Denmark (photo credit: European Energy), (top right): overhead trackers from HyPErFarm European project (photo credit: Fraunhofer ISE) , (center left): overhead semitransparent trackers in apple orchard in Bavendorf, Germany (photo credit: Fraunhofer ISE), (center right and bottom left): Jack's Solar Garden in Longmont, Colorado (Photo credit: NREL), (bottom right) NREL agrivoltaic testbed in Golden CO, U.S.A.

Even without adjustments to the standard Sun tracking algorithm, trackers provide more homogenous ground irradiance than equator-facing fixed tilt systems [61, 62], which can benefit plant productivity in certain seasons [56]. Lastly, a benefit of using trackers in inter-row type agrivoltaics (vegetation grown between rows of solar panels rather than beneath them) installations is that custom backtracking strategies can be used to avoid partial shading from crops. In this way, trackers can accommodate taller crops (e.g., tree crops, hedges, or greenhouse structures) than fixed tilt systems for inter-row type agrivoltaic projects. Casares De La Torre et al. [63] presents a possible analytical approach for avoiding shade from inter-row crops that have heights above the tracker torque tube.

The potential drawbacks of collocating PV energy and agricultural production can include higher installation and ongoing costs, lower PV production due to increased soiling [64], and soil erosion from dripping of water off of the PV module edge [65]. Trackers may reduce the extent of the latter disadvantages, specifically regarding their ability to reduce soiling effects and to partially control the distribution of precipitation.

Soiling refers to the accumulation of dust and dirt on the PV array – a process that may be accelerated when PV arrays are placed amidst agricultural activities [66]. Soiling has a strong dependence on tilt angle, with steeper PV arrays being less susceptible to soiling [67]. This is because a smaller effective area (compared to horizontal tilt) reduces the number of airborne particulates that can be deposited from the force of gravity. Therefore, an effective approach to mitigate soiling in agrivoltaic systems—and PV projects in general—is to stow trackers at steep tilt angles during the night (e.g., ≥55°), so long as structural safety is not compromised.

Sturchio et al. [68] observed that soil moisture levels in tracker installations have four distinct locations: directly below the PV array, the western drip edge, the eastern drip edge, and the area between trackers. The same study showed how grassland productivity correlates with soil moisture content and with the PAR received. In some agrivoltaic projects, a more homogenous soil moisture distribution may be desired. To this end, Elamri et al. [69] demonstrated how the soil moisture homogeneity below trackers could be improved by using a so-called ‘avoidance strategy’. The most successful strategy minimized rain interception by tilting the PV array about its angular limits (±50° in this case) during precipitation events. Although this strategy decreased the variation of rainfall distribution, such an approach may lead to excessive motor wear.

3 PERFORMANCE MONITORING AND EVALUATION

3.1 Instrumentation best practices

Well-designed sensor networks are important for monitoring the health of PV assets and for ensuring that production is fulfilling contractual obligations. The IEC 61724-1 standard [70] defines equipment and methods for monitoring the performance of PV systems, including bifacial tracker systems. The standard provides requirements for utility-scale systems (referred to as Class A requirements) and for rooftop and commercial systems (referred to as Class B requirements). Table 2 lists the irradiance and environmental measurements necessary to comply with Class A monitoring system requirements. The requirements are nearly the same for all non-concentrating PV system types except that monofacial PV systems do *not* require **rear plane-of-array irradiance** (RPOA) or albedo measurements, and fixed-tilt systems do *not* require inclination (tilt) measurements. Compared to conventional fixed tilt monofacial systems, the instrumentation in bifacial tracker systems requires additional considerations. The "Bifacial Option 1" set of measurements relies on the use of a transposition model to estimate RPOA, which can introduce significant uncertainties and result in differences depending on the model selected. Bifacial Option 2, which measures RPOA irradiance directly, is affected by uncertainties caused by the large spatial variability of RPOA irradiance. Methods to reduce these uncertainties are discussed in the sections below.

Table 2 – List of required irradiance and environmental measurements per IEC 61724-1 for fixed-tilt, tracker, monofacial and bifacial systems.

	IEC 61724-1 Class A		
Measurement	**Monofacial**	**Bifacial (Option 1)**	**Bifacial (Option 2)**
GHI	x	x	x
DHI		x	
Albedo		x	
POA Irradiance	x	x	x
RPOA Irradiance			x
Wind Speed and Direction	x	x	x
Back-of-module Temperature	x	x	x
Inclination (if system is tracker)	x	x	x

3.2 General Considerations for Irradiance Measurements

The placement of global irradiance sensors, including rear and front side POA and those installed horizontally (GHI), should be chosen to ensure they provide a representative view of the prevailing conditions in the field. This includes minimizing the unwanted effects of shadows cast by objects such as trees, power lines, and the like [71].

In large PV plants, periodic cross-checks of each irradiance sensor against redundant or reference devices are recommended to identify sensors that are either heavily soiled, faulty, mounted on stalled trackers, or out of calibration. Any sensor maintenance, including calibration activities, should be carried out to minimize downtime and interruptions to the sensors themselves. Methods for achieving this goal may include:

- replacement of faulty sensors with new or recalibrated units;
- provision of redundant or backup sensors with alternated calibration schedules in the laboratory;
- on-site checks with a reference instrument.

For Class A monitoring systems, irradiance sensors should be recalibrated once every two years, or more frequently according to manufacturer recommendations and considering specific environmental conditions and contractual requirements.

3.3 Front Side Plane-of-Array Irradiance

Front side sensors for measuring POA irradiance on trackers should be mounted such that they follow the movement of the tracker. In Class A monitoring systems, front side irradiance sensors must be inspected for misalignment and cleaned weekly. However, pyranometers with ventilation units may require less frequent cleaning because the constant air flow over the glass dome mitigates the effects of dust, frost, and snow. The IEA PVPS Task 16 indicates that conflicts of interest may arise if a single contractor is responsible for maintaining both high solar plant efficiency and high-quality irradiance data. This is because measurement errors caused by soiled pyranometers or wrong pyranometer installation can lead to an overestimation of the PV system's performance ratio [72].

Korevaar and Nitzel recently performed ray-trace simulations of 1P SATs to determine the optimal POA irradiance sensor positioning [73]. Their simulations showed that the annual cumulative irradiance across the POA of a SAT is nonuniform. Specifically, irradiance on the north and south ends of the front side POA were up to 2.5% higher than the overall average, while irradiance on the east and west edges of the front side POA irradiance were as low as 3.5% below the average. These results can be explained by the varying view factors along the front side of the array. For example, in the morning and afternoon, the east and west edges of trackers have an obstructed view of the sky due to surrounding trackers, alternating depending on the time of day. This concept of reduced POA irradiance due to an obstructed field of view is analogous to irradiance masking on fixed-tilt systems, which has been studied experimentally and theoretically [74].

Korevaar and Nitzel [73] used their simulated results to identify locations for front side POA irradiance sensors on SATs that are representative of the annual average. The recommended POA irradiance sensor positions are shown with the green rectangles in Figure 17. Note that these positions are located on an inner tracker and

that recommended sensor positions begin five modules away from the edge. Finally, it should be highlighted that field validation of these results remains an ongoing task.

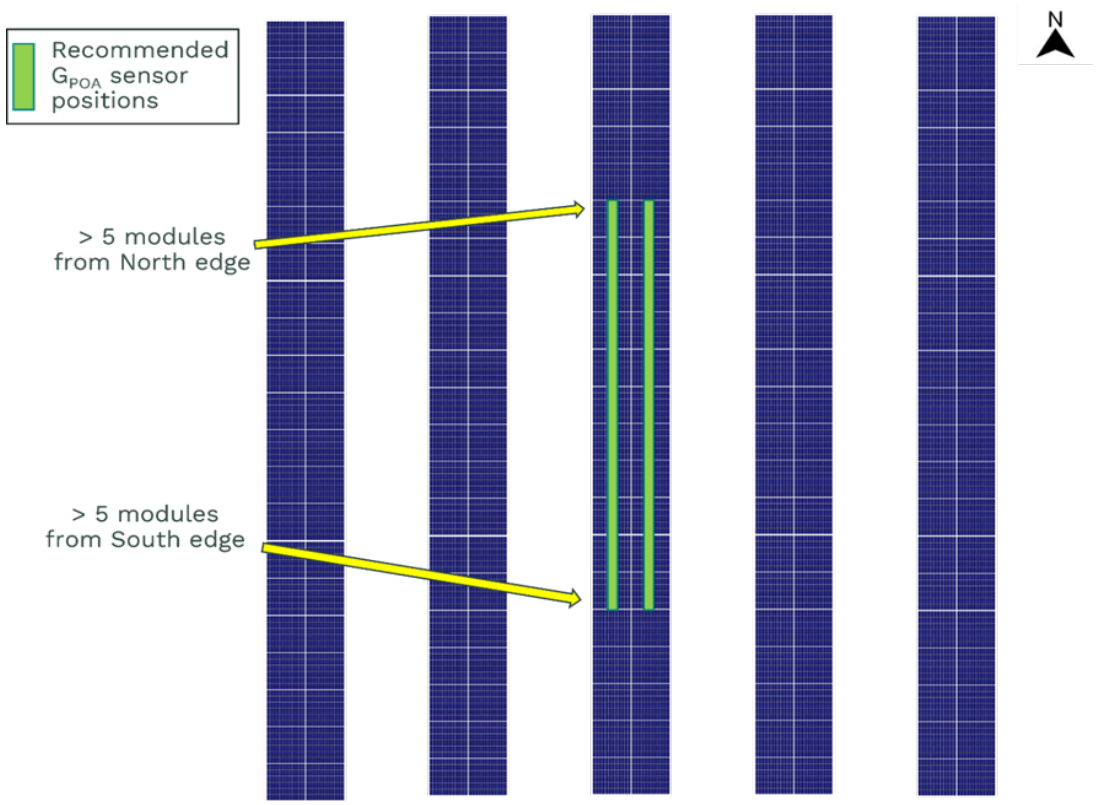

Figure 17 – Annotated aerial view of a 5-row SAT system. The green rectangles highlight POA irradiance sensor positions that are representative of the long-term average. Figure recreated from Korevaar and Nitzel 2023 [73].

3.4 Rear Plane-of-Array Irradiance

Determining the exact solar resource on the rear side of bifacial systems is challenging. Irradiance on the rear side of a PV array, varies spatially and temporarily depending on the diffuse light fraction (DHI/GHI), mounting structure, system layout, and ground surface properties [75]. The IEC 61724-1 standard provides the following guidance on the placement of RPOA irradiance sensors for both fixed-tilt and tracker systems [70]:

- ensure sensors are positioned to capture a comprehensive view of the conditions present on the array's rear side, while minimizing shading of the array;
- sensors should be mounted at the same tilt angle as the modules, directly on the module support structure, away from row ends, mounting posts, and other sources of localized shading or enhanced illumination phenomena;
- in areas where the terrain varies, employing an appropriate number of sensors and sampling methodology is necessary to capture these variations;
- since rear irradiance measurements may vary based on sensor position, particularly on inclined planes, using multiple sensors along the transverse line

of the module array (i.e., east to west in tracker systems) is recommended to better represent rear-side irradiance heterogeneity. This facilitates quantifying rear irradiance non-uniformity and calculating an effective average.

The IEC 61724-1 standard states that Class A bifacial PV systems must have three times the number of backside irradiance sensors as front side sensors. Figure 18 illustrates the correlation between the number of sensors and system size for Class A monitoring systems. For example, a 50 MWp system requires three front side POA irradiance sensors and nine RPOA irradiance sensors. This quantity of RPOA irradiance sensors, in conjunction with a judicious sampling methodology, can provide a detailed overview of RPOA irradiance variations throughout a PV plant.

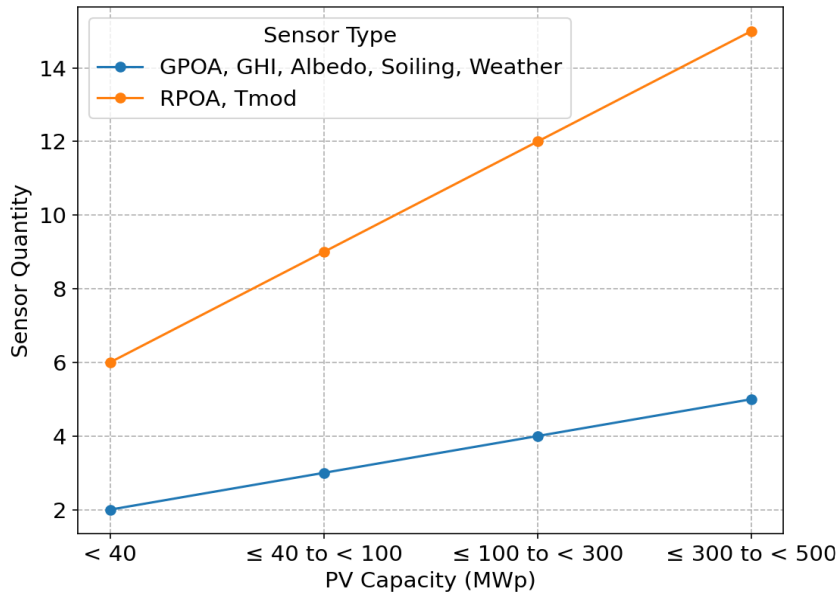

Figure 18 – Sensor quantities required for PV projects of various sizes to qualify as Class A per IEC 61724-1.

Although the standard stipulates the number of sensors to use within a PV plant and provides guidance on how to avoid measurement errors, it does not precisely specify where backside sensors should be mounted. This is because providing standardized guidance for every PV structure type and topography is difficult. Furthermore, the spatially non-uniform and time-varying nature of RPOA irradiance makes it challenging to identify small-area sensor positions that accurately represent the entire array.

Several research works have analyzed and proposed methods to obtain a representative value of RPOA irradiance using full-sized calibrated reference modules [76-78]. Although these studies indicate that reference modules can be used to accurately capture RPOA irradiance in all weather conditions, the use of bifacial modules as large-area sensors for irradiance measurements remains an emerging method for outdoor applications with no international standardization to date. Therefore, it is currently more common to use small-area sensors such as thermopile pyranometers or c-Si reference cells which have been in use for decades and are well codified in standards such as ISO 9060 [79].

Moreover, suitable RPOA irradiance sensor positions for 1P and 2P trackers have been investigated theoretically with ray-trace modeling [80-82], and empirically using

specialized measurement equipment on 1P trackers [83] and 2P trackers [80, 84]**.** The results from these studies have converged on the recommended RPOA irradiance sensor locations shown in Figure 19. These positions are recommended because it has been demonstrated that they best represent the full array area average, and they minimize bias in performance ratio calculations and capacity testing.

Figure 19A shows how RPOA irradiance sensors on SATs should always be installed at minimum 3–5 modules away from the north or south edge. This criterion applies to all SATs regardless of module mounting orientation (e.g., 1P, 2P, 3H). Figure 19B shows the recommended RPOA irradiance sensor positions for 1P systems while Figure 19C shows the recommendation for 2P systems. In both cases, it is advised to mount at least two RPOA irradiance sensors on the tracker: one sensor east of the torque tube, and the other to the west. Specifically, Figure 19B shows that RPOA irradiance sensors should be mounted halfway (50%) between an east/west edge and the center of the torque tube. This can typically be achieved on commercial trackers by fixing RPOA irradiance sensors to the transverse beams (purlins). The recommendation for 2P systems is similar to 1P except that RPOA irradiance sensors on 2P systems can be placed slightly closer to the east/west edges. Figure 19C shows that RPOA irradiance sensors on 2P systems should be mounted 40–50% of the distance between the east/west edge and the torque tube. Riedel-Lyngskær and Anderson, 2023 [82] showed that 40% is particularly recommended when 2P systems have a gap between the upper and lower modules.

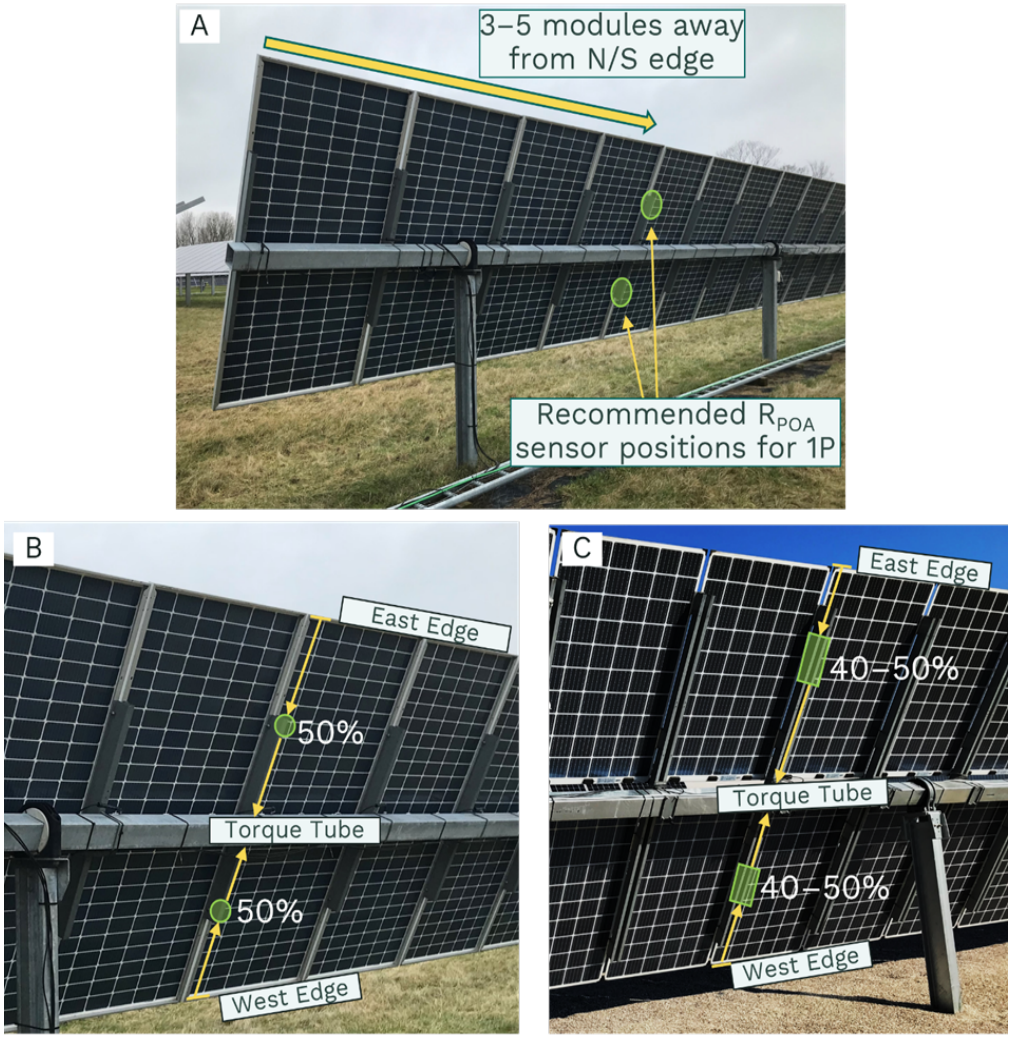

Figure 19 – (A) Visual example of avoiding north-south edge brightening effects on the back of trackers; a 1P SAT is shown here, but the guidance applies to other SAT designs. (B) Close-up of the recommended RPOA irradiance sensor positions for 1P SATs. (C) Close-up of the recommended RPOA irradiance sensor positions for 2P SATs.

3.5 Back-of-module temperature

Accurate **back-of-module temperature** (TMOD) measurements are challenging due to inter-module temperature nonuniformities [85] and due to difficulties of ensuring good thermal contact between the TMOD sensor and module surface [86]. For bifacial modules, TMOD sensors and cabling will inevitably shade part of the cell(s) that they are mounted to. The IEC 61724-1 standard states that TMOD sensors and wiring shall not obscure more than 10% of any given cell. This is reasonably easy to achieve when using typical large-format wafers (e.g., M10/M12) and when TMOD cabling is routed between cell gaps as shown in Figure 20**.** At typical back-to-front side irradiance ratios (i.e., when albedo < 0.3), such TMOD sensors are not likely to put a cell in reverse-bias and cause hotspots [87]. However, if operators of bifacial systems wish to perform

TMOD measurements without partially shading the rear side, the open-circuit voltage (VOC) of a calibrated reference module could be used to determine the equivalent cell temperature [77, 88, 89].

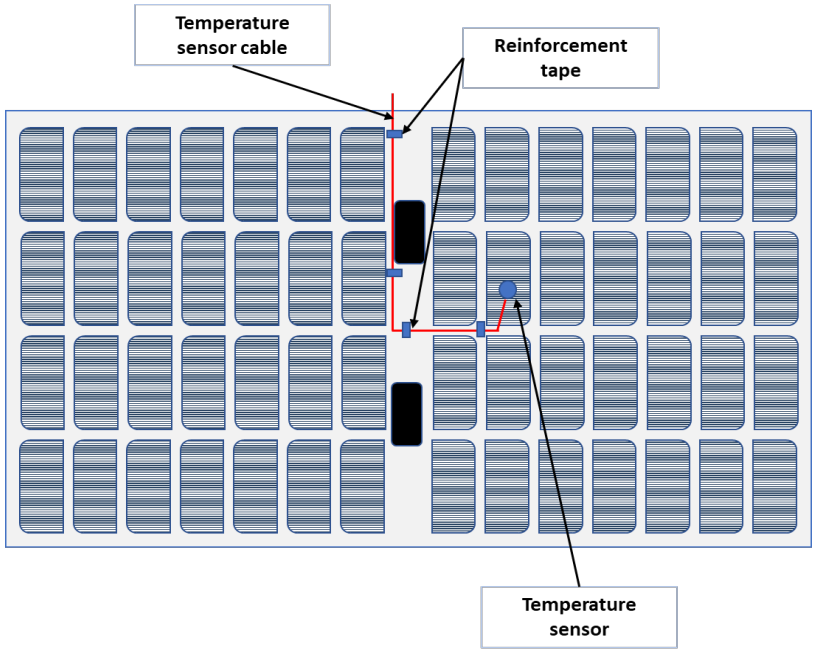

Figure 20 – Representation of back module temperature sensor positioning with minimal cell shading.

3.6 Wind speed and direction

Wind data is important for estimating module temperature (if not measured) and for correlating wind-related damage with high wind speed events. Compared to fixed-tilt projects, tracker projects require larger quantities of wind speed sensors (e.g., anemometers) because trackers rely on a wind-stow strategy to prevent dynamic resonances that can cause critical failures. Wind speed sensors for tracker control are typically connected to a network control unit (NCU), which sends centralized commands to individual tracker control units (TCUs) to stow during high wind speeds. One NCU is typically responsible for controlling approximately 200 TCUs, but the exact number is manufacturer specific. Wind direction measurements are also important for tracker projects because the tracker wind-stow angle may depend on wind direction. For example, some tracker designs stow by tilting into the prevailing wind direction.

High measurement accuracy of wind sensors is not critical when they are used for tracker control because the purpose is simply to detect whether the wind speed is above or below a threshold. Thoughtful placement of wind sensors is required in tracker projects to ensure that they do not shade the array and are not located adjacent to obstacles such as trees or transformers, that could affect the wind measurements. It is ideal to mount anemometers at, or close to, the standard 10 m height. However, such height is often not permitted due to municipal visibility requirements, especially when the PV plant is located near housing developments.

Wind speed measurements within large PV plants can vary widely. For example, Figure 21 shows one month of minute-level wind speed measurements from 9 anemometers within a 0.4 km^2 PV plant area located in Denmark. The lower frame of Figure 21 shows the difference between the highest and lowest wind speed reading within the plant. The range of measurements in this example sometimes exceeds 10 m/s, but 75% of the time, the agreement is within 3 m/s. Wind speed data sampling rates and processing methods of such wind speed data can vary among tracker manufacturers. It is important that PV plant operators understand their specific wind processing methods to assess if the NCUs are correctly implementing stow decisions.

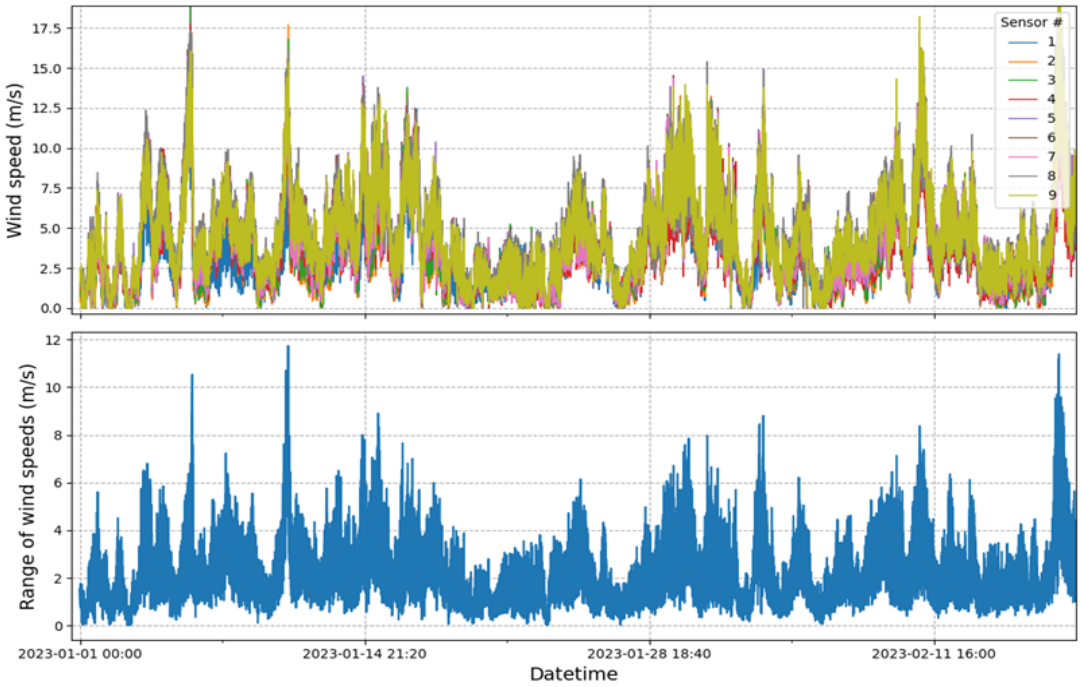

Figure 21 – Top) example 1-minute wind speed data from 9 sensors in a utility-scale tracker project in Denmark. Bottom) difference between the maximum and minimum measurement.

3.7 Inclination

Most commercially available TCUs have an inclinometer or accelerometer chip to measure the tracker tilt angle. Continuous monitoring of tracker tilt angle is important to ensure that the system follows its expected trajectory. Timeseries measurements of tilt angle also allow PV asset managers to quickly and confidently identify stalled trackers. However, utility-scale tracker projects often have hundreds and sometimes thousands of TCUs. Since it can be difficult to manage a database of this size for an entire project lifetime, some tracker projects may not have complete timeseries inclination data. If a tracker project does not have tilt angle measurements available, stalled trackers can still be identified from the PV energy production data using a method such as those presented in [90, 91]. However, these methods perform best

during clear sky conditions and may be cumbersome for some asset managers to implement. Therefore, onsite monitoring of tilt angle at the individual tracker-level is preferred.

An example check of tracker inclination is given in Figure 22. In the top frame, the tracker tilt reported by a TCU is compared to the modeled tilt for the site location, time of year, and GCR. The modeled tilt in this example was calculated using the Anderson and Mikofski algorithm [32] implemented in pvlib-python [92, 93]. The site modeled here is considered flat, so slope-aware backtracking was not used. The bottom frame of Figure 22 shows the difference between the measured and modeled angle. The magnitude of the error, for this 2P tracker, changes with time of day and with the phase of tracking. For example, the backtracking periods in the morning and afternoon show the largest error, while the lowest error is observed when the tracker is at the ±50° articulation limit. During the true tracking phase in the middle of the day, the deviation between measured and modeled angle is within ±1°, which is the accuracy stated by the tracker manufacturer. Some trackers are programmed to move in regular intervals of time, while others may move in irregular time intervals. Therefore, it is advantageous to know the specifics of the control algorithm when performing analysis such as the one shown in Figure 22.

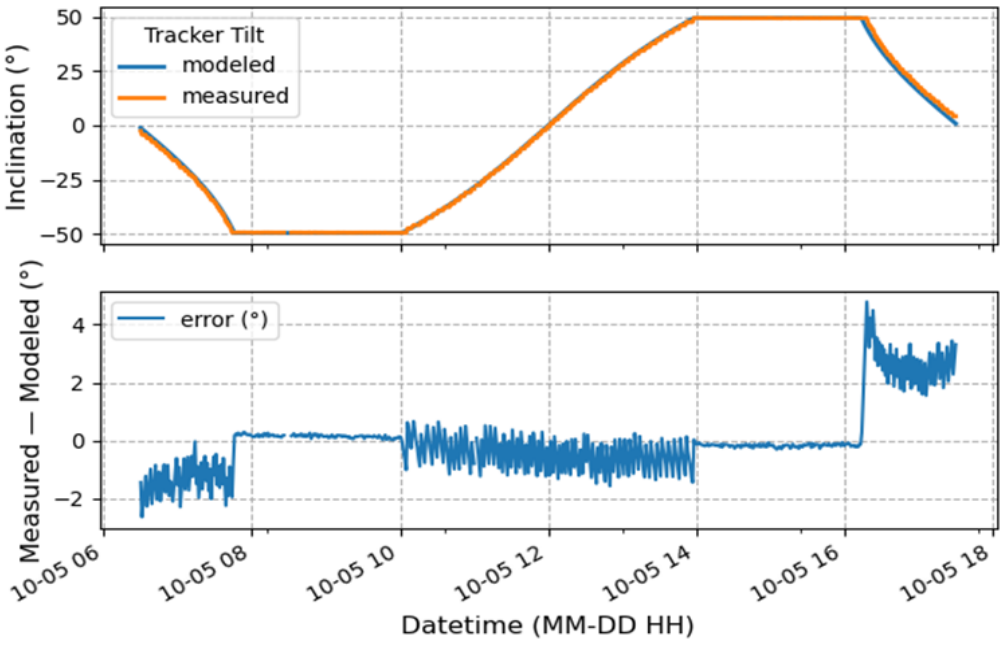

Figure 22 – Top) Example of modeled tracking angle of a commercial 2P tracker compared to measured angle. Bottom) Deviation between the measured and modeled angle.

3.8 Ground Albedo

Ground albedo is the reflectivity of the ground surface. It is a dimensionless quantity wherein albedo of zero represents a perfect absorber and albedo of one (or 100%) is a perfect reflector. Albedo is typically determined using two horizontal, spectrally flat pyranometers: one directed upwards towards the sky and the other

downwards towards the ground (Figure 23). The resulting albedo is calculated by dividing the output from the ground-facing pyranometer, which measures ground reflected horizontal irradiance, by the output from the sky-facing pyranometer, which measures global horizontal irradiance (GHI).

Broadband pyranometers have historically been used for albedo measurements, but when albedo data are used in bifacial PV applications, questions arise over whether spectrally selective instruments such as reference cells are more appropriate [77, 94, 95]. Because the spectrum of ground-reflected light is very different than the AM1.5G spectrum under which all terrestrial PV devices are calibrated, measurement errors up to 25% can occur if spectral effects are not accounted for—especially above vegetated surfaces such as grass. This property of spectral albedo lead Blakesley et al. [95] and Merodio et al. [96] to propose a hybrid albedometer, wherein the downward facing pyranometers is replaced by a Si reference cell to capture spectral effects. A pyranometer is still recommended as the upward facing device to avoid complicated angular corrections that would be necessary to apply to horizontal reference cell measurements. Figure 23 shows an experimental albedo measurement test stand at the U.S. National Renewable Energy Laboratory with broadband (pyranometers) and spectrally selective sensors (reference cells and photodiodes). The instrument pair to the left is a conventional upward and downward facing pyranometer set up for albedo measurements. Note the glare screen on the downward facing pyranometer to avoid direct light at low Sun angles. The center instrument is an upward and downward facing pair of Silicon reference cells, which have special interest for bifacial PV applications. A pair of upward and downward facing Silicon photodiodes are located to the right of the Silicon reference cells.

There are a number of standards and best practice guidelines that define albedo measurement protocols and methodologies for minimizing the measurement uncertainty thereof (e.g., ASTM E1918-21, ISO/TR 9901:1990, WMO 2018, IEC 61724-1:2021, [72]. For example, the ASTM E1918-21 standard aims to establish a replicable method for measuring solar reflectance across different materials and surfaces. While it offers a useful framework for comparative analysis, its focus does not directly address the unique requirements of bifacial PV systems. Namely, the short (0.5 m) measurement height and limited measurement duration make ASTM E1918-21 an unsuitable reference for albedo measurements in bifacial PV systems. On the other hand, the IEC 61724-1 standard [97] provides guidance for designing the mounting structure and placement of albedometers used specifically for bifacial PV applications. According to IEC 61724-1, albedo sensors should be installed at a minimum height of 1.0 m above the ground to provide an adequate field of view for capturing both the upwelling ground-reflected irradiance and downwelling global irradiance, while also allowing easy access for maintenance. This height requirement is in agreement with ISO TR 9901, which recommends heights of 1.5–2.0 m. Lastly, the fourth edition of the IEA PVPS Task 16 Best Practices Solar Radiation Measurements Handbook provides many further details and considerations for designing albedo measurement stands [72]. For example, this handbook provides insights on albedo instrumentation selection, design of measurement campaigns, quantification of shadow effects, spatial and temporal averaging approaches, measurements on sloping terrain, and other useful considerations.

Figure 23 – Experimental albedo measurement test stand with three different types of albedo sensors (Photo credit: NREL).

IEC 61724-1 states that albedo sensors should have an unobstructed view of the ground without shading from any nearby vegetation or obstacles within a ±80° viewing angle. This 160° field-of-view corresponds to a radius of 8.5 m around the albedometer when the sensor height is 1.5 m, and includes about 97% of the ground-reflected irradiance within full view of the downward facing instrument [75]. However, it is challenging (sometimes nearly impossible) to identify a 17.0 m diameter shadow-free zone within fenced meteorological station areas, or inside utility-scale PV plants where PV substructures are typically densely packed. Because of this difficulty, IEA PVPS Task 16 recommends a more conservative 5.0 m unshaded radius when the sensor height is 1.5 m [72]. Roughly 93% of the total ground-reflected light visible to the downward facing instrument is received within this 5.0 m radius. Furthermore, since some shadows under the albedometer are usually unavoidable, the authors state that measurements with significant shadows can be filtered out, depending on the impact to the long-term average albedo.

If there is significant variation in the ground surface within the bifacial PV site, multiple albedo sensors should be used to capture the variation and minimize uncertainty. IEC 61724-1 proposes one albedometer for every tilted irradiance sensor as a baseline for capturing possible variations—scaled according to Figure 18**.** Merodio et al. observed that the ground conditions at a PV site can be significantly different before and after construction, especially in vegetated sites [96]. In such cases, any albedo measurements performed during the pre-construction phase may not be representative of the PV site's albedo until several months after construction. This consideration has consequences for provisional acceptance certificate (PAC) testing,

or capacity testing, which are typically conducted shortly after commercial operation begins.

Modeling albedo is complex because it varies with wavelength, solar elevation angle, sky diffuse fraction, surface roughness, and surface moisture content [98]. Most of these fundamental albedo properties have already been studied in detail by other research fields (e.g., remote sensing and climate science). With the commercial rise of bifacial PV, the PV community's particular research focus has been understanding how albedo modeling techniques, various data sources, and measurement uncertainty affect bifacial energy yield estimations.

A valuable work on modeling albedo is that of Tuomiranta et al. who benchmarked 20 different albedo models to ground measurements at 26 sites [99]. On a global average, they found that modeling albedo with in-situ-measured data, instead of literature-derived constants, reduces mean absolute error by 22%, 29%, and 39% with constant, univariate, and bivariate models, respectively. An in depth comparison of albedo from five publicly available sources (NSRDB, MERRA-2, MODIS-MCD43GF, CMSAF, and ERA5) was conducted by Gueymard et al. [100] who compared the satellite-derived albedo products to each other on a global scale, and to ground measurements at select sites. They found that these five sources had the largest differences at high latitudes (>40°N). They also compared MERRA-2 and MODIS to 10 years of ground measurements at a desert location in Nevada, USA and found that MERRA agreed remarkably well to measurements whereas MODIS was 0.03 lower on average. Marion created a large database of ground-based albedo measurements from nearly 40 locations and published the work as an open-access data set to enhance the PV community's understanding of albedo [50]. Marion notably found that a default albedo value of 0.2 is reasonable, except when a location experiences snow, or is a desert location in which case the albedo is usually greater than 0.2.

The question of how albedo measurement uncertainty and temporal variations can impact bifacial energy yield estimates has been addressed by several authors. The effect of monthly versus annual average albedo values in bifacial performance simulations was studied by Patel et al. [101]. Their global simulations showed small differences (<1%) in energy yield when annual average or monthly average albedo was used and suggested that an annual constant albedo is suitable for most bifacial PV simulations—except for sites with snow. Darling et al. [102] ran PVsyst simulations of 34 sites, and for each site, used albedo data from three satellite-based sources as well as ground-based measurements. From this exercise the authors revealed that the sensitivity in annual energy production with respect to annual albedo variation is ~1/6 (0.167). In other words, a 0.06 change in albedo causes a 1% change in simulated bifacial energy yield [102]. This result is in close agreement with that of Lara-Fanego et al.[103] who used a similar methodology, as well as GUM principles (Guide to the Expression of Uncertainty in Measurement), to show that bifacial energy yield deviates by ~1.5% when the uncertainty (k=2) of the albedo measurement is ±0.03 and the albedo itself is roughly 0.2 [103]. Finally, Merodio et al. [96] used GUM principles and showed that the sensitivity of bifacial energy yield due to albedo changes with climate, ground surface, substructure type (fixed vs. tracker), and installation conditions (GCR and inverter loading). This work found that the sensitivity coefficient of bifacial energy yield due to albedo is between 0.18–0.30.

4 PERFORMANCE MODELING AND YIELD ASSESSMENT

4.1 Performance Modeling Methods

Modeling the basic performance of any PV system involves estimation of the plane-of-array (POA) irradiance, module/cell temperature, and application of an electrical model that estimates the resulting IV curve or maximum power point for the module string or array connected to the inverter. Other modeling steps include calculation or application of derate factors such as soiling and snow loss, reflection losses, current mismatch, wiring losses, etc. Tracked bifacial systems are more complicated due to the changing tilt angle over the day and the fact that both front and rear irradiance need to be estimated to calculate total POA irradiance.

Estimating tracking angles for commercial trackers requires knowledge of the maximum tilt angle of the tracker and information about the specific tracking algorithm being used (e.g., true tracking vs. backtracking). Simulating more advanced tracking algorithms such as diffuse-response, self-cleaning, hail-response, or wind-response, requires details from the tracker manufacturer. Typically, such details are not available and standard algorithms are used along with derates to account for deviations.

Methods for simulating front and rear side irradiance are well documented elsewhere [4]. Two predominant techniques find application in various models and software for bifacial PV system simulation—**View Factors** and **Ray Tracing** [104]. A third method based on GPUs is also discussed.

View factors

This modeling approach, using View factors (VF) technique [105], focuses mainly on calculating the rear-side irradiance on the PV modules. VF represents the fraction of irradiance leaving one surface and reaching another. Table 3 lists performance modeling applications that are based on the VF method. The use of VF simplifies calculations and reduces the simulation time due to its 2D assumption. In this approach PV rows are assumed to be long, minimizing the impact of edge effects. It is applicable for single or multiple rows of PV modules by calculating rear-side irradiance for each row to assess the radiation profile on the PV module. VF assumes isotropic radiation, where intensity remains consistent for all angle-of-incidences (AOIs). To address disruptions from shadows for ground-reflected radiation on the PV module's back side, the ground area can be divided into segments, applying VF separately and summing the results for resultant ground-reflected irradiance. (Figure 24).

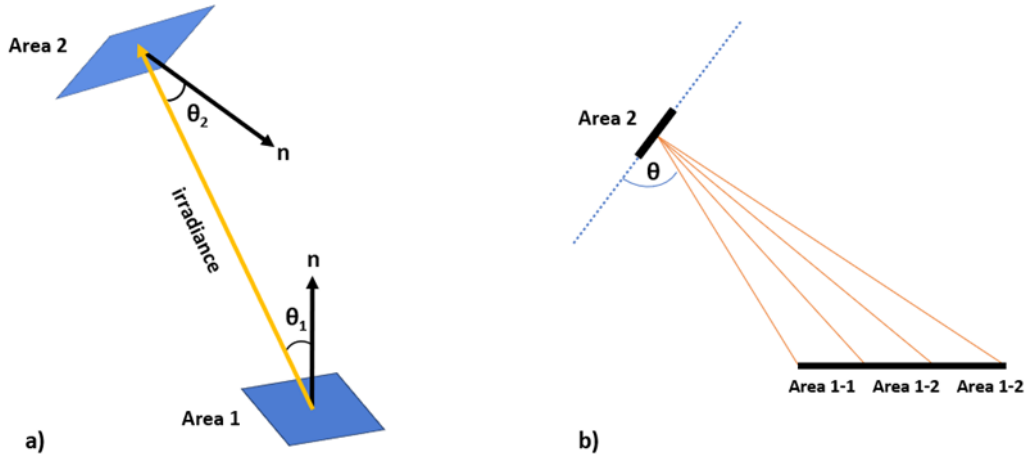

Figure 24 – (a) VF principle, b) VF Segmentation

Table 3 – Selected performance models that are based on the view factor method.

Feature	SAM (System Advisor Model) / bifacialVF	PVsyst	PVsol	PVFactors	Trifactors
Single-Axis Tracking	x	x	x	x	x
Dual -Axis Tracking	x	x	x		
View factors principle	x	x	x	x	x
Backtracking	x	x			
Slope-awareness	x				
3D near shading analysis		x			
Agrivoltaic features	x				
Owner/Developer	NREL	PVSyst SA	Valentin Software	SunPower	INES
Commercial (C)/Open Source (OS)	OS	C	C	OS	C

Ray Tracing

Ray tracing is a computer graphics rendering technique that accurately models scene lighting by tracing the path of light from the view camera through the 2D pixel plane into the 3D scene and back to light sources. It realistically replicates reflections,

refractions, shadows, and indirect lighting, generating realistic images. There are various types of ray tracing methods:

- **Forward Ray Tracing** traces light from the source to the object for accurate coloring but this method requires many rays to accurately represent scenes, making it numerically expensive.
- **Backward Ray Tracing** introduces rays only from points where irradiance calculations are desired (e.g., points on the rear surface of the bifacial modules). Ray tracing follows these rays, including a specified number of bounces, until they reach a light source (e.g., the sky or Sun).
- **Hybrid Ray Tracing solutions** which involve both methods to improve efficiency and accuracy.

Table 4 lists performance modeling simulators that are based on the ray-tracking method. Most simulators use the Backward Ray Tracing to calculate incident irradiance on the PV modules as shown in Figure 25 using bifacial_radiance [106].

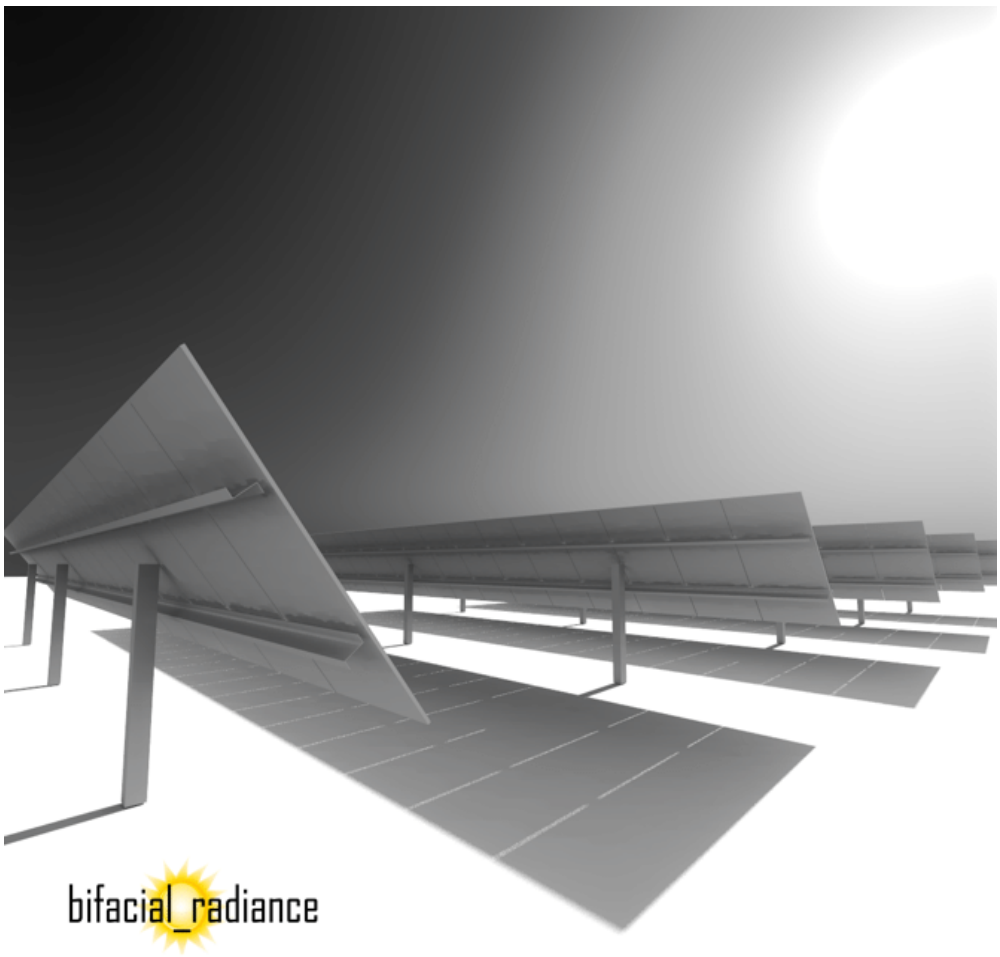

Figure 25 – Image generated using bifacial_radiance, a backward ray-tracing simulator (Image credit: J. Alderman).

Table 4 – Simulators based on Ray Tracing principles.

Simulator features	Simulator				
	bifacial_radiance	**PVNOV**	**MoBiDig**	**DUET**	**Energy Yield Simulation**
Single-Axis Tracking	x	x	x	x	x
Dual-Axis Tracking	x				
Ray Tracing principle	x	x	x	x	x
Backtracking	x	x			
Slope-awareness	*				
3D near shading analysis	x	x		x	x
Owner/Developer	NREL	EDF	ISC	SUNLAB	IMEC
Commercial (C), Open Source (OS), Internal (I)	OS	I	C	I	I

* Can be added from pvlib-python

GPU-based 3D view factors

The 3D view factor method makes use of high-resolution 3D graphics processing units (GPUs) to estimate the distribution of light (irradiance) on the rear side of bifacial solar arrays. The assessment of the view factors involves a rendering of specific spherical projections at various module locations. The core distinction between this high-resolution 3D view factor method and the traditional ray-tracing technique lies in their respective units of analysis. Ray-tracing relies on rays as its fundamental unit, meticulously simulating the behavior of light as it interacts with various surfaces. While this approach is renowned for its accuracy, it is also known for its substantial computational expense. In contrast, this 3D view factor method pivots on pixels as the primary unit of analysis. This critical shift not only introduces enhanced simulation flexibility but also significantly improves the efficiency of GPU utilization. By leveraging pixels, this approach takes full advantage of GPUs' capability to process extensive pixel data concurrently. This optimizes overall performance and diminishes the computational load, offering a reasonably accurate yet resource-efficient alternative to ray-tracing. Notably, the method's efficiency enables simulations to be conducted using simple and affordable computer setups, underscoring its accessibility and practicality. The view factors for irradiance components necessitate a detailed assessment at discrete points across the photovoltaic (PV) array, as illustrated in Figure 26.

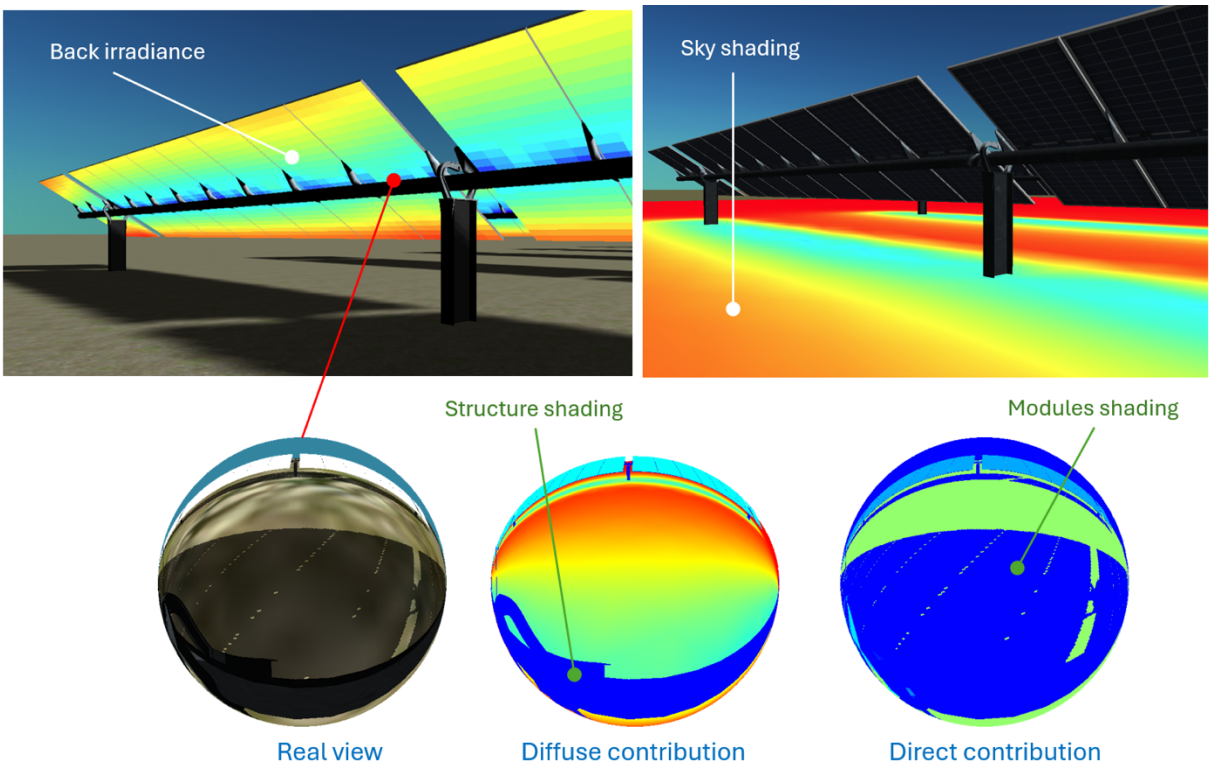

Figure 26 – View factors and their use in the irradiance evaluation of SATs in LuSim.

The 3D view factor method has been implemented by independent research institutions or companies, most notably by TNO (BigEye [107]), University of Twente (VR4PV [108]), and LuciSun (LuSim [109, 110]). The high-resolution 3D view factor method for estimating irradiance distribution represents a promising advancement in solar energy simulation. However, this method is still undergoing development and requires further validation. Currently, validation efforts are underway within the framework of several international research projects (SERENDI-PV, SYMBIOSYST).

4.2 Model intercomparison and round robin

Many of the models described in section 4.1 have not been thoroughly compared and validated in a consistent manner. To assess the consistency of results between various models, participants were invited to simulate a series of design scenarios. Unlike other modeling comparisons run by the PV Performance Modeling Collaborative (PVPMC) [111], this was not based on real systems with measured performance data. Instead, scenarios were defined that provided enough information to set up a model and simulate performance. Then all of the participant results were analyzed to measure the consistency of these models.

Scenario descriptions and process

Six scenarios are described in Table 5. Participants were given a year of hourly-averaged irradiance and weather data, module specifications (spec sheet and PAN

file), and array specifications. For computationally expensive models the option to just simulate five representative days was offered. The modeled system consisted of five tracker rows. Participants were asked to simulate each scenario and return hourly results of (1) front and rear POA irradiance, (2) module temperatures for the South, middle, and North modules of the center row, (3) modeled tracking angles, and (4) DC string power for the middle row.

Table 5 – Scenario definition for modeling intercomparison.

Scenario	GCR	Albedo	Hub Height	Module Configuration	Ground surface
S1	0.4	0.2	1.5 m	1-Up portrait	Horizontal
S2	**0.25**	0.2	1.5 m	1-Up portrait	Horizontal
S3	0.4	**0.5**	1.5 m	1-Up portrait	Horizontal
S4	0.4	0.2	**3.5 m**	1-Up portrait	Horizontal
S5	0.4	0.2	1.5 m	1-Up portrait	**10% grade* down to the East**
S6	0.4	0.2	1.5 m	1-Up portrait	**10% grade* down to the SW**

Note: A 7th scenario of a 2P system was originally included but was removed from the final analysis for simplicity.

Scenario S1 was considered a reference case with each of the other scenarios changing just one design variable (bolded in Table 5).

Participants and models used

Nine participants submitted results. They used the models listed below for their calculations. Note that the models are listed in a random order to anonymize which participant ran each model:

- **Irradiance models**: Perez transposition, bifacial_radiance, pvlib-python infinite sheds, pvlib-python PVfactors, internal model.
- **Module/cell temperature models**: Sandia Array Performance Model (SAPM), PVsyst, pvlib-python pvsyst_cell, internal model.
- **PV power models**: CEC, Heydenreich, 2-diode model from PVMismatch, SolarFarmer, PVsyst, BIGEYE

Two of those participants only ran the five representative days due to their models being computationally expensive. Figure 27 displays the irradiance profiles on those days. The days were chosen to represent different seasons including both clear and partly cloudy conditions. Participant 9 only submitted front and rear POA irradiance and is therefore not included in plots below of module temperature, tracking angles, and string power.

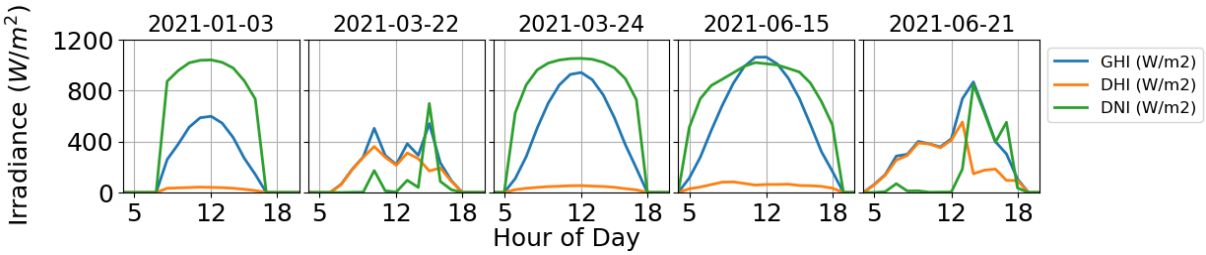

Figure 27 – Irradiance profiles for the five representative days

Participant results

Figure 28 shows that the total energy predicted by each participant varied by as much as +5% to -10% from the mean of the results for each scenario. The accuracy of each model cannot be known since these scenarios were generated to test whether models consistently were able to predict the effects of changing certain input parameters. But this range in the results indicates that there is a need for further model improvement, validation, and standardization.

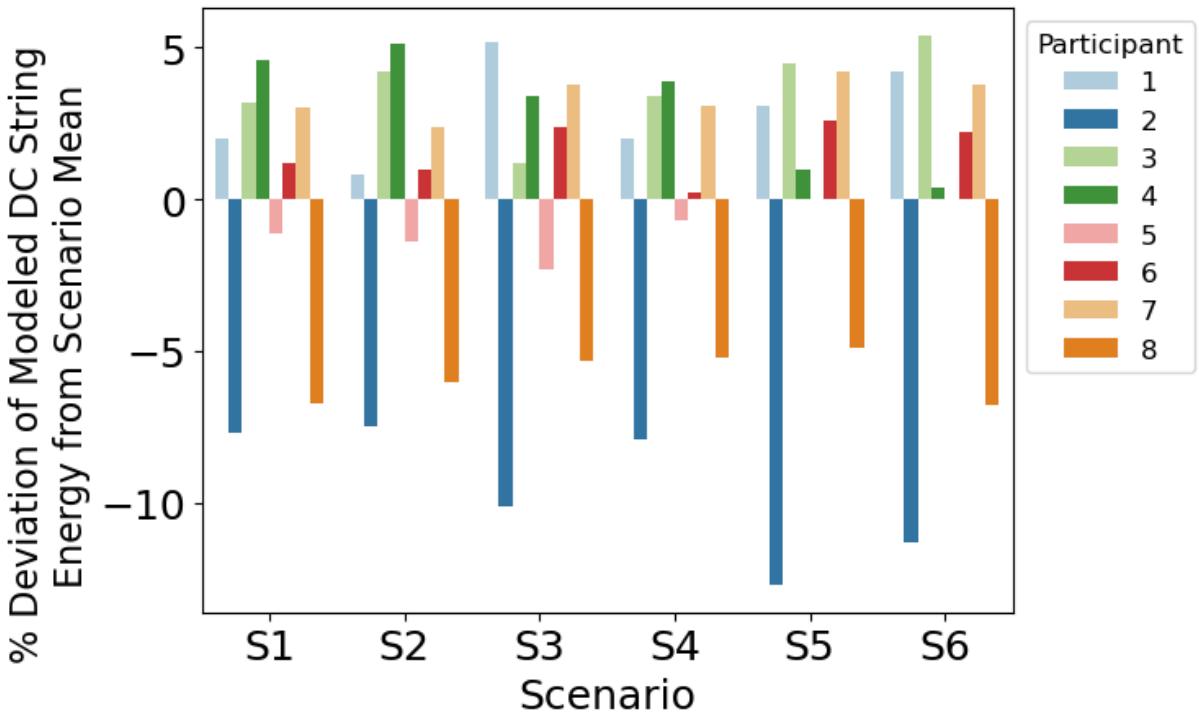

Figure 28 – Percent differences in total energy for each participant calculated from the mean of each scenario.

The figures below show greater detail on how various model outputs varied between participants on four of the five representative days. Figure 29 plots the front plane-of-array irradiance on the center module for all the participants. It is interesting that even for this standard model calculation there are still some participants with occasional outlier results.

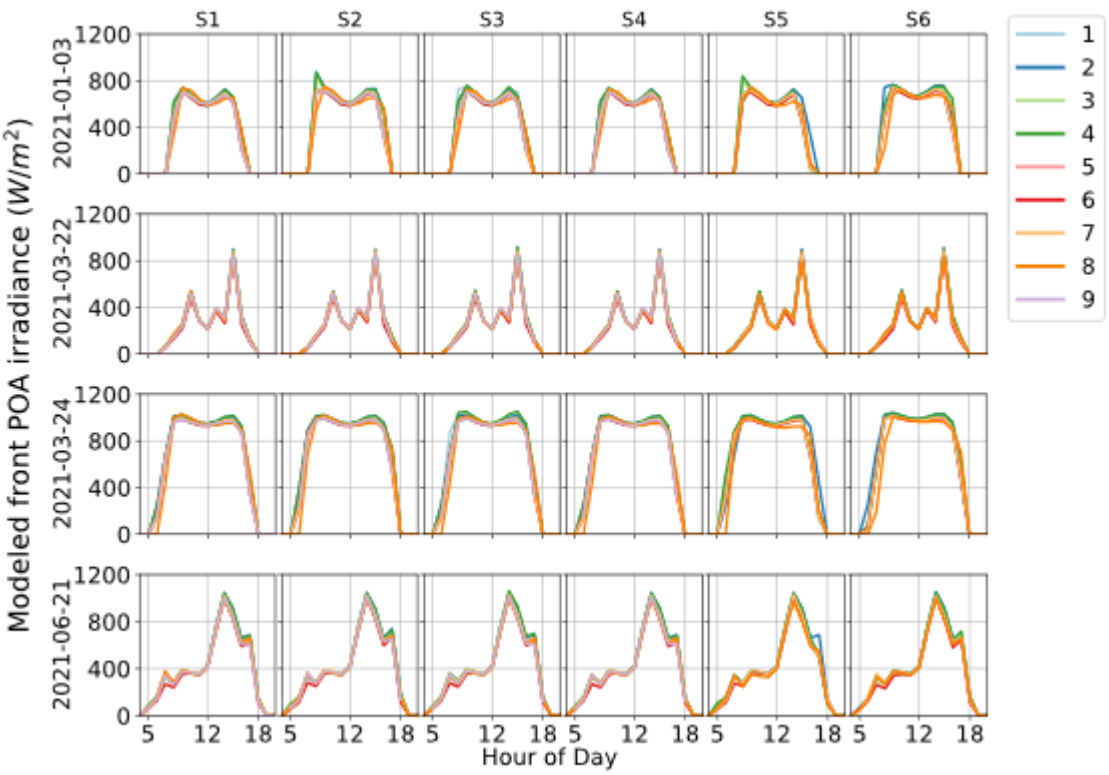

Figure 29 – Comparison of daily profiles of modeled front plane-of-array irradiance for the center module.

Figure 30 plots the rear plane-of-array irradiance for the center module for all participants. This quantity shows significantly more variability between the participants. Seven out of the nine participants ran models that were able to distinguish performance differences (edge effects) between the modules on the north, center, and south modules in the row. While it is encouraging to see that the rear irradiance appears higher for all participants in the high albedo scenario (S3), it is notable that the shape and magnitude of rear irradiance daily profiles differ quite significantly (by as much as ~100% difference) between participants. This result suggests that more work is needed to ensure that rear irradiance model calculations are validated against actual field measurements (e.g., [104]).

Figure 31 plots the module temperature for the center module for all participants. There is a large range in module temperature results between the participants. Some of this variation is due to the range in rear POA irradiance. Runs with higher rear POA irradiance sometimes result in higher module temperatures, but not always. For example, module temperatures on 3/24/2022 and 6/21/2022 show that participant #2 predicted the highest temperatures but did not have the highest rear irradiance.

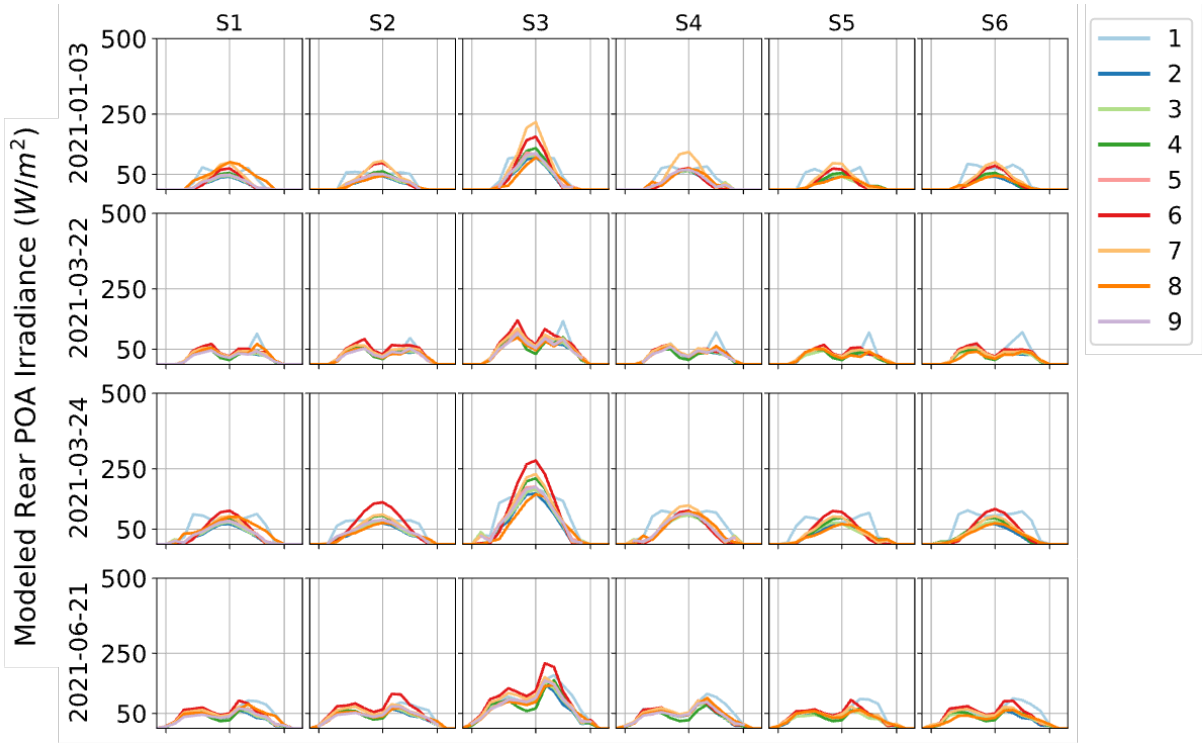

Figure 30 – Comparison of daily profiles of modeled rear POA irradiance for center module. Rows are for selected days and columns represent scenarios S1-S6.

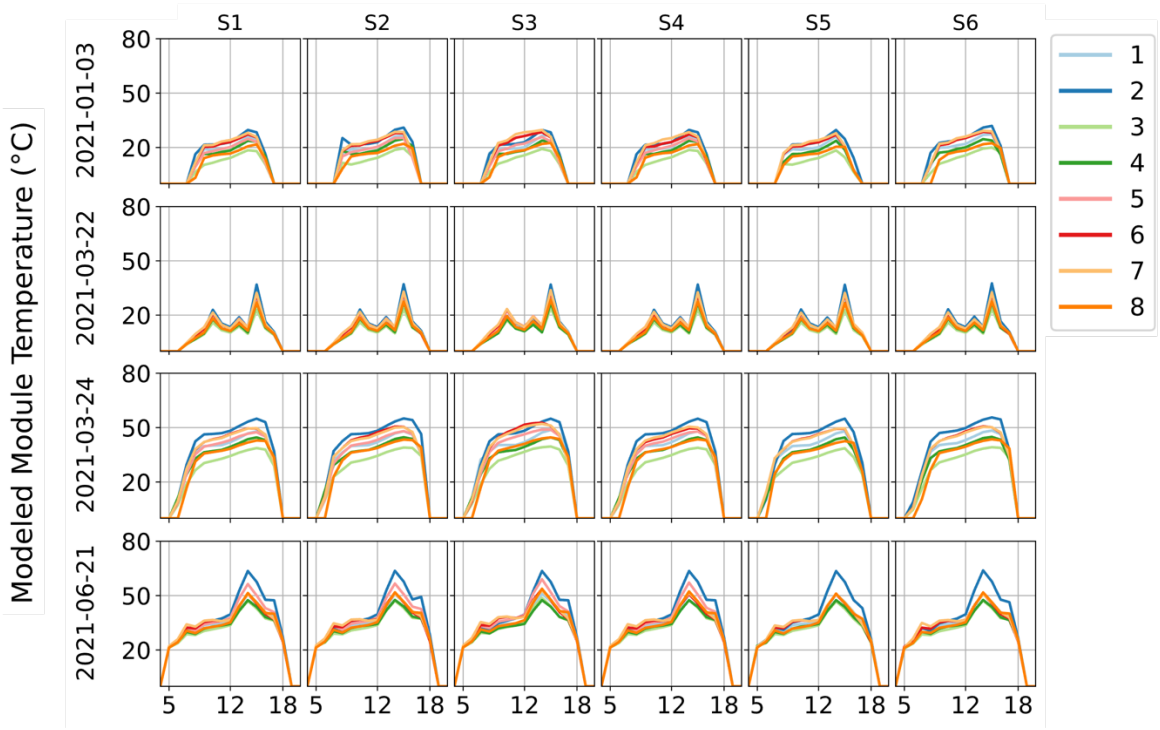

Figure 31 – Comparison of daily profiles of modeled module temperature for center module. Rows are for selected days and columns represent scenarios S1-S6.

Figure 32 plots the tracker rotation angles from each of the participants. This figure also shows that this is an area that likely needs some attention as not all the participants calculated the same tracker angles. A closer look at S5 and S6 scenarios shows that there is more disagreement among participants during the backtracking periods in the morning and evening, which is likely due to these scenarios including a sloped ground surface.

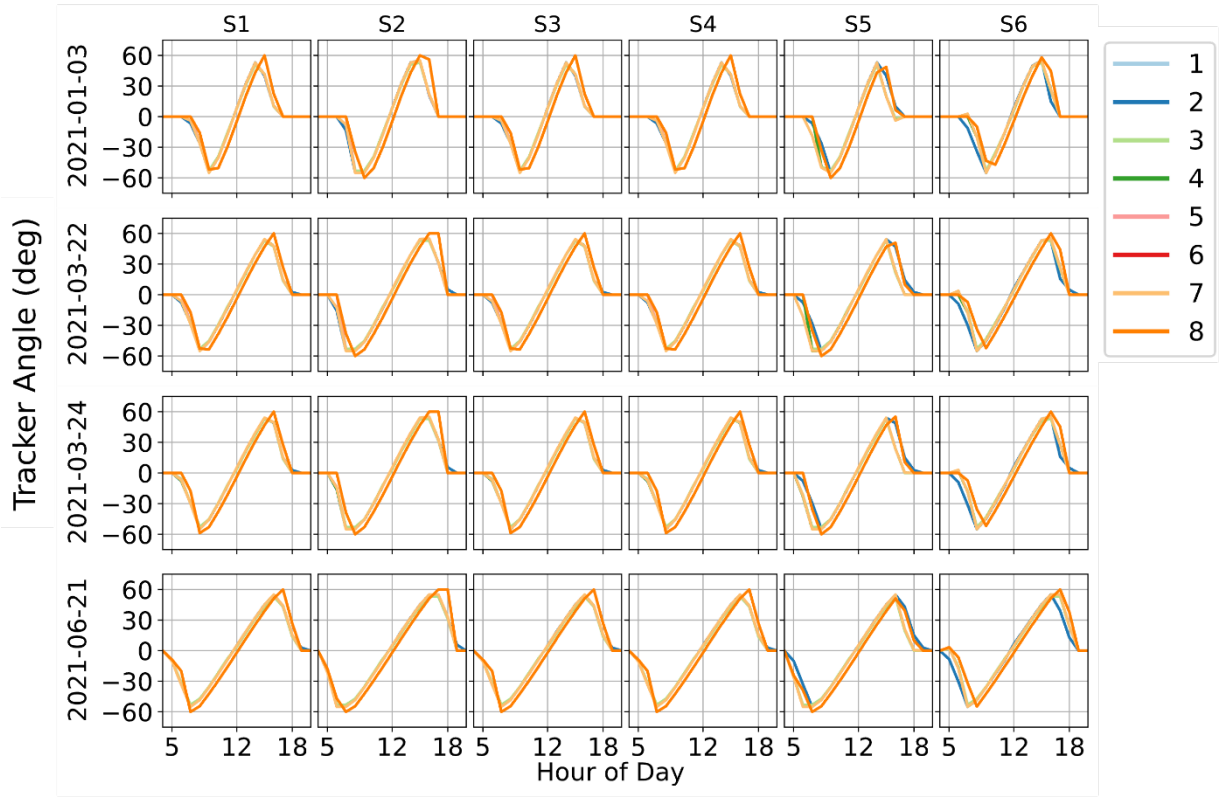

Figure 32 – Comparison of daily profiles of modeled tracker rotation angles. Rows are for selected days and columns represent scenarios S1-S6.

Figure 33 plots the modeled string DC power from all participants who submitted these results. Since DC power is a function of all the previous intermediate results, all the variations between participants are evident in DC power. For example, participants who estimated high module temperatures, also usually estimated higher rear side irradiance and lower DC power.

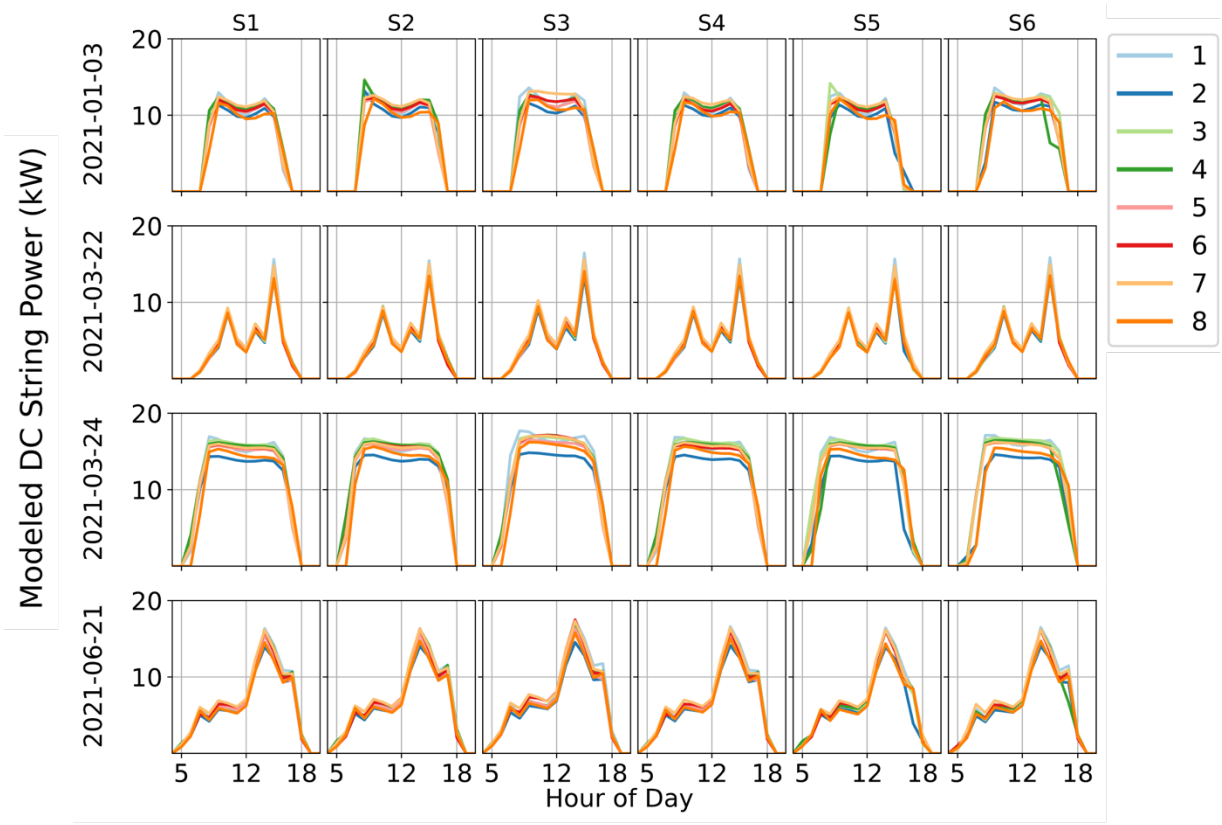

Figure 33 – Comparison of daily profiles of modeled DC string power. Rows are for selected days and columns represent scenarios S1-S6.

5 RELIABILITY CONSIDERATIONS

Relative to a fixed tilt PV system, trackers add additional points of failure and moving components which may require additional maintenance. The additional energy gain from tracking must exceed the additional expense of tracking system installation and maintenance. Thus, the reliability of a tracker system is an important consideration in the design and development of PV systems. It is notable that in reviewing the literature on solar tracking reliability, there is very little published work in this area and much of the information is gathered from conversations with industry and system owners. In this section aspects of tracker reliability and failures including common failure modes, effects of failure, reliability metrics, and testing standards are examined.

5.1 Failure modes

Failure modes may be classified as either **intrinsic** (i.e., caused by a failure of the tracking system) or **extrinsic** (i.e., caused by outside forces). Intrinsic failure modes are caused by a failure in some component of the tracking system, they may be mechanical or electrical in nature. Extrinsic failures can be caused by extreme weather events or inadequate site testing (e.g., geotechnical surveys, pull and load tests of foundations, etc.).

Intrinsic failure modes

For systems where trackers or tracker blocks require communication with a central control unit to maintain tracker function or accuracy, the communication system may become a point of failure. Communication system failures may result from broken wireless (e.g., Zigbee, Wi-Fi) or wired (e.g., RS-485, Ethernet) interfaces. Failures in communication systems may cause a loss of tracking accuracy or a pause in the tracking.

Single-axis trackers determine their rotation angle through means such as a feedback mechanism to maximize irradiance or production of the system, or they may track based on astronomical calculations of the position of the Sun given the tracker location and time. In either case, inputs to the tracking algorithm may be inaccurate or interrupted and cause a failure of the tracking system.

Mechanical failures within a single-axis tracker may reduce tracker reliability. Tracker systems require mechanical components that are not present in fixed-tilt systems including components such as motors, gearboxes, and bearings. Furthermore, as these components become worn and degrade in performance, they may stress other mechanical systems. For example, a gearbox may begin to seize and require additional torque from the motor, thereby straining the motor and reducing its life.

Extrinsic failure modes

Tracker failures may also be caused by external forces in the outdoor environments in which they operate. For example, wind-blown sand may be forced into tracker components and reduce their lifespan. Assuming proper installation techniques, electronics and control enclosures rated for outdoor use are typically resistant to

particulates, but rotation bearings, motors, encoders, and gearboxes may accumulate these abrasive particles. Constant movement with abrasive particles will cause higher wear on these components.

The primary extrinsic failures in SAT systems are caused by wind. A correctly designed SAT system should be designed to withstand common high wind events, frequently moving to a safe “stow” position to minimize wind loading. However, it is possible that a large wind gust may cause a failure in some portion of a SAT system including the modules, module clips, mounting rails, etc. These extreme wind conditions may cause catastrophic failures which tear modules from their mounting.

Consistent winds, even if not extreme, may cause instability in the SAT system as air interacts with the PV modules along the long torque tubes. The module-air interactions are affected by the relative angle of the PV module to the wind as well as the tracker’s location within the field. Combined, these effects may cause torsional instability which can lead to high torque oscillations in the SAT torque tube, leading to failure of the system. These events may be commonly known as “torsional galloping”, “flutter”, or “torsional divergence”[112, 113].

5.2 Effects of failure and design considerations

Tracker failures result in the tracker getting stuck or possibly moving to the wrong position, however such failures rarely cause the PV array to become disconnected. Therefore, during most tracker failures, the PV module array keeps generating electricity. This means that the economic effects of such failures are less than reliability issues affecting power generating components such as inverters, combiners, and modules. To illustrate this effect, the performance of a SAT PV system in Albuquerque, New Mexico USA was simulated, including various failure scenarios. It was assumed that the tracker suffered one failure that caused the system to stall and remain fixed in the orientation it was at when it failed, and the number of days that the tracker remained stuck was varied. For each failure duration 200 random times during the year when the failure started were sampled. Figure 34 shows the percent of annual energy lost as a function of the number of days that the tracker remained stalled. Energy losses tend to increase with the duration of failure, but so does the range of losses, depending on when the failure occurs. It is interesting to note that for a small fraction of the points, the percent of lost energy lost is negative. This is explained by the tracker stalling near horizontal during a period characterized many diffuse days.

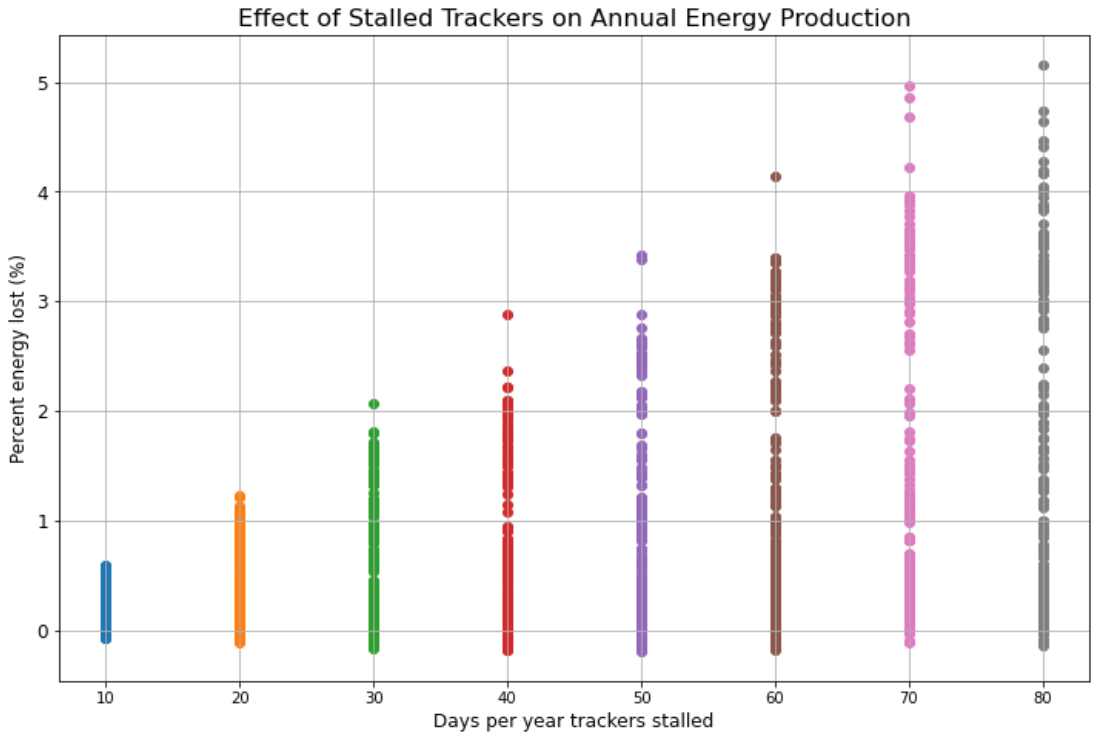

Figure 34 – Percent of annual energy lost due to tracker stalls of different durations simulated in Albuquerque, NM, U.S.. Each point represents one of 200 randomly selected times when the stall initiated at each increment of duration.

A range of issues affecting tracker performance and reliability were identified in the tracker owner/operator survey. Figure 35 ranks these in order of importance from the survey responses. Mechanical failures, particularly with slew drives and motors, were frequently cited as contributing factors.

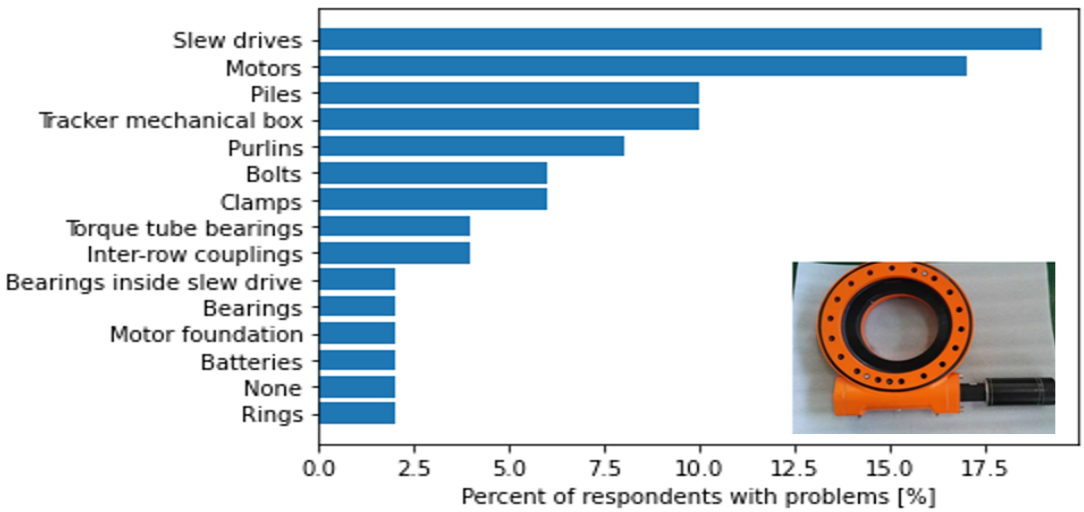

Figure 35 – Percentage of surveyed owner/operators reporting tracker component failures. The bottom right corner shows a picture of a standard slew drive, which was reported as the most common failed component.

Figure 36 ranks technical challenges, such as tracker misalignment and row-to-row shading despite the use of backtracking, experienced by users. Notably, in regions with northern winter climates, battery-powered tracker solutions demonstrated poor performance, highlighting a specific vulnerability in adverse weather conditions. These findings underscore the multifaceted nature of tracker reliability challenges, encompassing mechanical, environmental, and electrical factors that must be addressed to enhance overall system resilience and performance.

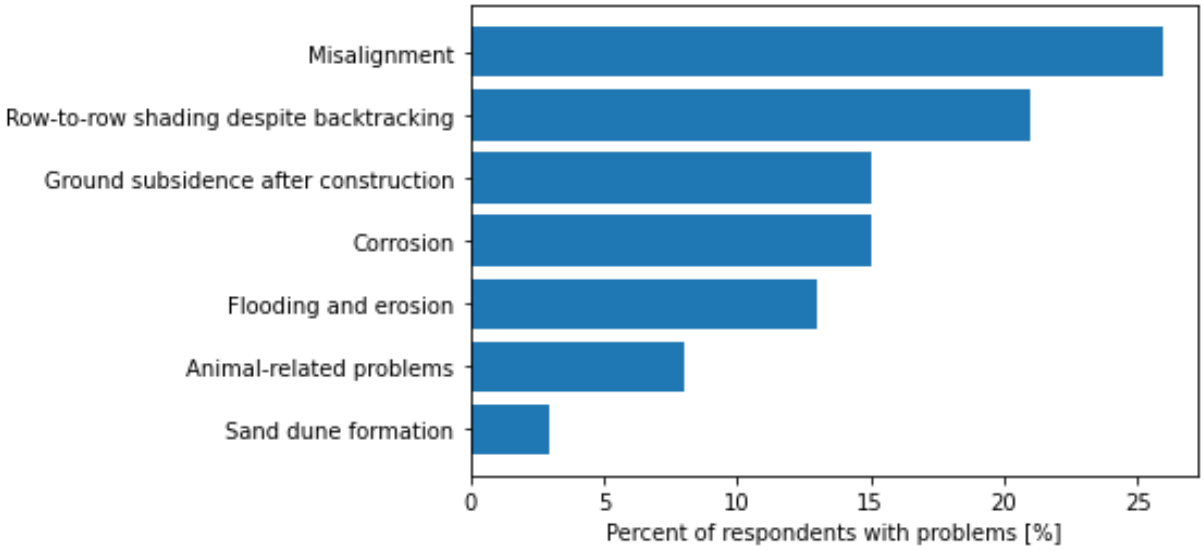

Figure 36 – Percentage of owner/operators surveyed that reported problems with their systems.

6 TECHNICAL AND FINANCIAL OPTIMIZATION

Several different technical approaches have been described in the previous chapters, all addressing the opportunities for optimization of specific Key Performance Indicators (KPI) such as:

- Technology selection according to terrain conditions and (extreme) weather conditions,
- O&M cost reduction through reliability considerations and associated risk mitigation,
- Area utilization through optimized system layout,
- Energy yield improvement through albedo enhancement and advanced tracking algorithms,
- Reduction of uncertainty in yield estimates through improved monitoring and advanced irradiance modeling

But to perform an overall optimization and an associated decision on which technology and options to prioritize, it is not sufficient to just use indicators such as Yield/Capex or LCOE comparisons as these methods will not capture the true value creation of the various options.

A best practice approach to a technical and financial optimization, includes a full financial model (FM) reflecting the overall value of the project as seen by the investor/owner.

The main elements in such a model and the impact of the above specified KPI's on the model output will be discussed further below.

6.1 LCOE

The complex financial evaluation of bifacial tracker systems is a strong justification for the ongoing efforts in Task 13 Subtask 2 "Performance and Durability of PV Applications". Given that decisions regarding the construction of green or brown field power plants are often made based on narrow margins, it is crucial to ensure the highest possible accuracy in the simulation of dynamic scenarios that govern PV tracker bifacial gains. International tools and experts in yield simulation benefit from these validation efforts, particularly in the context of financial analysis as shown in the following sub-sections.

In financial analysis of power plants, two commonly used metrics are the levelized cost of electricity (LCOE) and net present value (NPV). LCOE serves as an internationally recognized benchmark for making financial decisions in power plant projects, enabling relative comparisons of new components, system types, or specific arrangements. However, LCOE analysis faces limitations when evaluating bifacial tracker solar power plants. Firstly, the assumptions used in LCOE calculations, such as future energy prices, discount rates, and system lifetimes, may not accurately reflect the unique characteristics of bifacial tracker systems. Secondly, the availability of CAPEX and OPEX data for bifacial tracker systems can be challenging, limiting access to specific information. Additionally, some static LCOE calculations may not adequately consider the temporal variability of bifacial gain, influenced by system layout factors like

the ones addressed in the round-robin exercise (albedo, pitch, etc.). This underscores the importance of Task 13 Subtask 2 “Performance and Durability of PV Applications” in addressing these limitations. The individual components of LCOE calculations are including in the image below, with bifacial tracker relevant remarks highlighted in each subsequent subsection.

Lifecycle cost
Costs during system operation

$$LCOE_{nom} = \frac{\left(CAPEX_{PV,total} + \sum\left[\frac{OPEX(t)}{(1+WACC_{nom})^t}\right] - \frac{ResValue}{(1+WACC_{nom})^N}\right)}{\sum\left[\frac{Yield(0)(1-Degradation)^t(Availability)}{(1+WACC_{nom})^t}\right]}$$

Lifetime energy production
Energy yield during system operating time

T	lifetime	ResValue	residual value of the PV system after its lifetime
N	economic lifetime of the system	Yield	energy produced
$CAPEX_{PV, total}$	investment	Degradation	degradation rate
OPEX(t)	annual operation expenditure in year t	Availability	percentage of the power plant’s operation
$WACC_{nom}$,	nominal weighted average cost		

6.2 Energy Yield

Obviously, the overall yearly energy generation is the main driver in value creation and all initiatives to increase this estimate through any of the mentioned KPI’s will be directly reflected in the energy generation part of the FM.

In this context the total energy yield as given mainly by the size of the project, is decisive. For projects where the sizing of the project is limited by availability of land, it’s possible to increase the size of the project by reducing the inter-row spacing at the expense of specific energy generation. Especially for tracker projects, this optimization exercise is important, since a low deployment density will have a positive impact on the specific production, which is the main selling point of the tracker supplier. To the disadvantage of such a technology focused optimization approach, it’s often seen that the project value for an area constraint project is higher when the inter-row spacing is reduced and the project size increased, even if this strategy compromises the achievable specific production.

In general, for all specific yield optimization strategies analyzed, the impact (cost adders) on O&M activities needs to be included in the CAPEX and OPEX section of the FM to enable optimization scenarios to be analyzed.

6.3 Revenue

Only in very simple business models, where all electricity generation will receive a flat Feed-In-Tariff or an energy sales price based on a flat-rate PPA, the yearly revenue

can be found by multiplying the annual generation by the annual sales price. In general, the revenue will not only reflect the overall level of the wholesale electricity price, but also the expected profile in hourly spot prices. This hourly breakdown determines the revenue directly as for a merchant sale, a Contract-for-Difference support scheme or indirectly for fixed price PPA where the price has been determined through an analysis of the time-of-production vs. expected spot prices in the specific market, but where this market risk has been transferred to the PPA taker.

The complexity refers to the character of the actual duck-curve, which reflects the inability of a PV generator to follow the demand for electricity and the associated oversupply of PV electricity during noon in summer which eventually will introduce low to negative electricity prices for the PV generated energy. This cannibalization effect where increased deployment of solar PV eventually will erode the revenue potential, is expected to significantly increase over the coming decades, with associated forecasted value factors (defined as average annual electricity value of the PV generated electricity divided by the average annual wholesale electricity price in the market) in the range of 50-70% to be expected.

With value factors in this range and with the indicated spread in estimates, it's obviously a difficult task to calculate the lifetime revenue from a PV plant with low uncertainty by yearly assumptions only. Alternatively, it may be required to analyze the revenue on an hourly basis where the modeled hourly generation profile for the specific tracker system and the specific yield enhancement methodology must be matched with an hourly spot price forecast under the same meteorological conditions as the resulting revenue calculation is an essential part of the financial modeling and scenario building. Since the generation profile from a tracker project in general matches the consumption to a higher degree than for fixed tilt systems, this analysis constitutes an essential part of the valuation of the project as compared to fixed tilt systems.

6.4 Capex

The total capex for the planned PV-tracker installation is mostly based on specific quotations from suppliers whereby necessary information on supplier bankability and details on technology specific impact on O&M or overall project sizing (area utilization) associated with different technology choices can be assessed.

The part of capex associated with cost of grid access and grid compliance, might introduce a separate optimization track, where different options for grid capacity assignment might impact not only the grid related Capex (scaled by the cost of AC-equipment and transformers, which may be available in narrow capacity ranges per unit, introducing step-changes in the capex) but also the available grid capacity introducing (voluntary) curtailment due to insufficient grid access or non-firm grid capacity agreements allowing the grid-operator to reduce the output of the plant during periods with grid congestion.

A best practice optimization analysis needs to consider various options for sizing of AC-equipment and the amount and certainty of the grid-capacity to be contracted impacting the potential curtailment of energy generation during specific hours (which might reflect hours of either high or low electricity value).

6.5 OPEX

Most items in the category of OPEX will not depend on the specific tracker technology that is selected. These cost items include land lease/property tax, bookkeeping/audit/bank charges, monitoring/telecom, onsite power consumption, O&M charges, including spare parts/component replacement, grid fees/balancing cost/generation of origin certificate administration, commercial and technical asset management and decommissioning cost/guarantee cost. Inflation profiles must also be assigned to each item, as well as to the sales price of electricity.

6.6 Financials

Further to complete the FM, details on the assumed debt financing (type of loan, leverage, maturity, interest rate) as well as depreciation per cost category and tax rate/tax credit must be specified. Although these financing conditions may not reflect the specific technology, it's also clear that the ability to obtain attractive financial conditions will depend on the bankability status of the suppliers, which then indirectly will influence the investor appetite to sign contracts with a less known supplier or an innovative/experimental technical solution.

Both exchange rates and interest rates which are given by the world-wide macroeconomic conditions, establish the ultimate conditions for any investment decision in the field of renewable energy plants, which most likely will be more decisive for an investment decision than the outcome of any technology-based optimization exercises. Also fundamental in determining the feasibility of a potential investment decision, is the target internal rate of return (IRR) that the investor/owner expects to obtain in the current market conditions (reflecting alternative investment opportunities in i.e. the stock or bond market).

6.7 Optimization

While knowing the investor target IRR, it's possible to compile all information collected per scenario into a series of annual cash flow. This cash flow series consists of the yearly revenue less the yearly expenses as detailed in the OPEX section, but also following subtraction of depreciation, financing cost and tax expenses.

The net present value of this cash flow by the investor target IRR will then reflect the equity value of the project and by subtracting the total project Capex, the expected profit for the investment in question is determined.

Although any profit above zero does reflect a positive business case, the decision by the project developer to go forward with the project (final investment decision, FID), will need to consider the total uncertainty in the estimated profit as well as the overall risk profile of the project. The key performance indicator then becomes the profit/capex, where a high-risk project will require a higher expected KPI value compared to a medium to low risk project where investments may be attractive also for low profit/capex project opportunities.

Although technology decisions may be made based directly on KPI's reference to the technical gain and cost, best practice optimization will need to reflect scenario building and financial modeling to assess the ultimate value creation on a project level for each of the analyzed technical options.

7 CONCLUSIONS

Photovoltaic systems using bifacial modules and single-axis trackers currently dominate the utility scale PV market in many regions of the world. However, there are still many technology-specific and site-specific factors that need to be investigated to optimize the performance of these systems.

Key areas where improvements are needed include:

- **Tracking algorithms**: Tracking companies avoid sharing details about how their specialized tracking algorithms work and therefore it is difficult to evaluate their performance and assess whether they add sufficient value to the bifacial technology or to a particular project. Developers interested in new tracking algorithms are encouraged to deploy multiple sets of trackers each running different algorithms at a site for a test period to help decide which one to use for the life of the plant. Side-by-side comparisons at the same site are necessary to validate industry claims of potential yield increases.
- **Albedo enhancement**: It is not yet clear whether the use of albedo enhancers, such as geosynthetics, will ever be economically feasible, but early studies have shown some promising results. Continuing research into low-cost, durable materials and optimal placement strategies will help determine if albedo enhancement becomes standard practice.
- **Response to extreme weather**: The ability of trackers to respond to rare, extreme weather conditions should be standardized. According to our owner/operator survey, there is a significant risk that a tracker will not respond appropriately to such an event. While these events are rare, their consequences are very impactful.
- **Capacity tests**: While the standardization of monitoring for bifacial tracked PV systems has improved significantly in recent years, there are still serious challenges for completing capacity tests on these systems due to factors such as high dc/ac ratios, periods of cloudy weather, and uncertainty in row-to-row shading and yield predictions.
- **PV performance models**: Yield prediction (performance) models for bifacial tracked systems need to be improved. Our round robin model comparison carried out on six scenarios demonstrated up to ~100% difference between rear side irradiance predictions between different models and participants. Also, predictions for module temperatures and even tracking angles were alarmingly variable between different participants. More high-quality, validated datasets are needed for model developers to ensure that models are more consistent.
- **Reliability**: There is very little literature on the reliability and durability of single-axis tracker systems. Longitudinal studies of different tracker technologies across different climates need to be supported. Such studies are important for optimizing the design and operation of tracked PV plants.

The use of bifacial modules and trackers for agrivoltaic systems is especially exciting because if it can be shown to be feasible, it could make available a vast amount of land for renewable energy generation and help many smaller countries benefit from PV

energy without sacrificing land for agriculture. A major challenge will be how to reduce the design complexity and variations for such applications to take advantage of standardization, high throughput manufacturing, and global supply chains to lower the cost. This will be difficult since it appears that every crop and site may present unique constraints for an agrivoltaic system, making it difficult to create standard system designs and operational strategies. Tracking systems will have an advantage since they can automatically adjust the amount of light reaching the crops.

REFERENCES

[1] "International Technology Roadmap for Photovoltaic (ITRPV)," VDMA, 2024, vol. 15th Ed.

[2] C. D. Rodríguez-Gallegos *et al.*, "Global Techno-Economic Performance of Bifacial and Tracking Photovoltaic Systems," *Joule,* vol. 4, no. 7, pp. 1514-1541, 2020/07/15/ 2020, doi: https://doi.org/10.1016/j.joule.2020.05.005.

[3] G. J. M. Janssen *et al.*, "How to maximize the kWh/kWp ratio: simulations of single-axis tracking in bifacial systems," presented at the 35th European Photovoltaic Solar Energy Conference and Exhibition (EU PVSEC), Brussels, Belgium, 2018.

[4] J. S. Stein *et al.*, "Bifacial Photovoltaic Modules and Systems: Experi- ence and Results from International Research and Pilot Applications," International Energgy Agency - Photovoltaic Power Systems Programme, 2021, vol. IEA-PVPS T13-14:2021.

[5] T. Dullweber *et al.*, "PERC+: industrial PERC solar cells with rear Al grid enabling bifaciality and reduced Al paste consumption," *Progress in Photovoltaics: Research and Applications,* vol. 24, no. 12, pp. 1487-1498, 2016, doi: https://doi.org/10.1002/pip.2712.

[6] T. Dullweber and J. Schmidt, "Industrial Silicon Solar Cells Applying the Passivated Emitter and Rear Cell (PERC) Concept—A Review," *IEEE Journal of Photovoltaics,* vol. 6, no. 5, pp. 1366-1381, 2016, doi: 10.1109/JPHOTOV.2016.2571627.

[7] D. Panico, P. Garvison, H. Wenger, and D. Shugar, "Backtracking: a novel strategy for tracking PV systems," in *The Conference Record of the Twenty-Second IEEE Photovoltaic Specialists Conference - 1991*, 7-11 Oct. 1991 1991, pp. 668-673 vol.1, doi: 10.1109/PVSC.1991.169294.

[8] D. Weinstock and J. Appelbaum, "Optimization of Solar Photovoltaic Fields," *Journal of Solar Energy Engineering,* vol. 131, no. 3, 2009, doi: 10.1115/1.3142705.

[9] P. Vanicek and S. Stein, "Simulation of the impact of diffuse shading On the yields of large single axis tracked PV-plants," presented at the 24th European Photovoltaic Solar Energy Conference, Hamburg, Germany, 2009.

[10] *UL 2703: Mounting Systems, Mounting Devices, Clamping/Retention Devices, and Ground Lugs for Use with Flat-Plate Photovoltaic Modules and Panels*, UL, 2015.

[11] *UL 3703: Standard for Solar Trackers*, UL, 2015.

[12] *IEC 62817: Photovoltaic systems - Design qualification of solar trackers*, IEC, 2014.

[13] A. Awasthi *et al.*, "Review on sun tracking technology in solar PV system," *Energy Reports,* vol. 6, pp. 392-405, 2020/11/01/ 2020, doi: https://doi.org/10.1016/j.egyr.2020.02.004.

[14] Y.-M. Saint-Drenan and T. Barbier, "Data-analysis and modelling of the effect of inter-row shading on the power production of photovoltaic plants," *Solar Energy,* vol. 184, pp. 127-147, 2019/05/15/ 2019, doi: https://doi.org/10.1016/j.solener.2019.03.086.

[15] S. Ong, C. Campbell, P. Denholm, R. Margolis, and G. Heath, "Land Use Requirements for Solar Power Plants in the United States," National Renewable Energy Laboratory, 2013, vol. TP-6A20-56290.

[16] A. Barbón, C. Bayón-Cueli, L. Bayón, and V. Carreira-Fontao, "A methodology for an optimal design of ground-mounted photovoltaic power plants," *Applied Energy,* vol. 314, p. 118881, 2022/05/15/ 2022, doi: https://doi.org/10.1016/j.apenergy.2022.118881.

[17] S. V. Pelt, A. B. Worden, and A. Assal, "Optimal mounting configuration for bifacial solar modules on single axis trackers," in "White Paper," Game Change Solar 2018.

[18] F. Bizzarri, "La Silla PV Plant: Innovative Bifacial PV Plant at La Silla Observatory in Chile," presented at the Bifi PV, Konstanz, 2017. [Online]. Available: http://npv-workshop.com/fileadmin/layout/images/Konstanz-2017/9__F._Bizzarri_ENEL_Innovative_tracked_bifacial_PV_plant_at_la_Silla_observatory_in_Chile_.pdf

[19] D. Valentín, C. Valero, M. Egusquiza, and A. Presas, "Failure investigation of a solar tracker due to wind-induced torsional galloping," *Engineering Failure Analysis,* vol. 135, p. 106137, 2022/05/01/ 2022, doi: https://doi.org/10.1016/j.engfailanal.2022.106137.

[20] A. Roedel and S. Upfill-Brown, "Using dynamic wind analysis and protective stow strategies to lower solar tracker lifetime costs," in "White Paper," NextTracker 2018.

[21] N. Straub, W. Herzberg, A. Dittmann, and E. Lorenz, "Blending of a novel all sky imager model with persistence and a satellite based model for high-resolution irradiance nowcasting," *Solar Energy,* vol. 269, p. 112319, 2024/02/01/ 2024, doi: https://doi.org/10.1016/j.solener.2024.112319.

[22] GCube, "Hail No! Defending solar from nature's cold assault," in "Q4 Report," 2023.

[23] R. F. Fuentes-Morales *et al.*, "Control algorithms applied to active solar tracking systems: A review," *Solar Energy,* vol. 212, pp. 203-219, 2020/12/01/ 2020, doi: https://doi.org/10.1016/j.solener.2020.10.071.

[24] N. Al-Rousan, N. A. M. Isa, and M. K. M. Desa, "Advances in solar photovoltaic tracking systems: A review," *Renewable and Sustainable Energy Reviews,* vol. 82, pp. 2548-2569, 2018/02/01/ 2018, doi: https://doi.org/10.1016/j.rser.2017.09.077.

[25] D. O. Papathanasiou and M. Schmela. (2021) Market Survey Solar Trackers 2021. *Taiyang News*.

[26] N. T. Katrandzhiev and N. N. Karnobatev, "Algorithm for Single Axis Solar Tracker," presented at the International Scientific Conference Electronics, Sozopol, Bulgaria, 2018.

[27] T. Tudorache and L. Kreindler, "Design of a Solar Tracker System for PV Power Plants," *Acta Polytechnica Hungarica,* vol. 7, 1, pp. 23-39, 2010.

[28] A. Al-Othman *et al.*, "An experimental study on hybrid control of a solar tracking system to maximize energy harvesting in Jordan," *Solar Energy,* vol. 263, p. 111931, 2023/10/01/ 2023, doi: https://doi.org/10.1016/j.solener.2023.111931.

[29] W. F. Marion and A. P. Dobos, "Rotation Angle for the Optimum Tracking of One-Axis Trackers," National Renewable Energy Laboratory, 2013, vol. NREL/TP-6A20-58891.

[30] K. Passow, J. Falls, and K. Hunt, "Sensitivity of PV Plant Performance to Tracker Error," in *2019 IEEE 46th Photovoltaic Specialists Conference (PVSC)*, 16-21 June 2019 2019, pp. 0659-0662, doi: 10.1109/PVSC40753.2019.8980662.

[31] E. Lorenzo, L. Narvarte, and J. Muñoz, "Tracking and back-tracking," *Progress in Photovoltaics: Research and Applications,* vol. 19, no. 6, pp. 747-753, 2011, doi: https://doi.org/10.1002/pip.1085.

[32] K. Anderson and M. Mikofski, "Slope-Aware Backtracking for Single-Axis Trackers," NREL, 2020, vol. Technical Report NREL/TP-5K00-76626.

[33] M. Leung *et al.*, "Tracker Terrain Loss Part Two," *IEEE Journal of Photovoltaics,* vol. 12, no. 1, pp. 127-132, 2022, doi: 10.1109/JPHOTOV.2021.3114599.

[34] K. S. Anderson and A. R. Jensen, "Shaded fraction and backtracking in single-axis trackers on rolling terrain," *Journal of Renewable and Sustainable Energy,* vol. 16, no. 2, 2024, doi: 10.1063/5.0202220.

[35] K. Rhee, "Terrain Aware Backtracking via Forward Ray Tracing," in *2022 IEEE 49th Photovoltaics Specialists Conference (PVSC)*, 5-10 June 2022 2022, pp. 0029-0030, doi: 10.1109/PVSC48317.2022.9938554.

[36] K. Anderson, "Maximizing Yield with Improved Single-Axis Backtracking on Cross-Axis Slopes," in *2020 47th IEEE Photovoltaic Specialists Conference (PVSC)*, 15 June-21 Aug. 2020 2020, pp. 1466-1471, doi: 10.1109/PVSC45281.2020.9300438.

[37] D. Keiner, L. Walter, M. ElSayed, and C. Breyer, "Impact of backtracking strategies on techno-economics of horizontal single-axis tracking solar photovoltaic power plants," *Solar Energy,* vol. 267, p. 112228, 2024/01/01/ 2024, doi: https://doi.org/10.1016/j.solener.2023.112228.

[38] A. Dobos, "Improved Tracking Schemes for Half-Cut PV Modules," presented at the 2022 PV Performance Modeling Collaborative (PVPMC) Workshop, Salt Lake City, 2022.

[39] K. Anderson and S. Aneja, "Single-Axis Tracker Control Optimization Potential for the Contiguous United States," in *2022 IEEE 49th Photovoltaics Specialists Conference (PVSC)*, 5-10 June 2022 2022, pp. 1-6, doi: 10.1109/PVSC48317.2022.9938629.

[40] C. D. Rodríguez-Gallegos, O. Gandhi, S. K. Panda, and T. Reindl, "On the PV Tracker Performance: Tracking the Sun Versus Tracking the Best Orientation," *IEEE Journal of Photovoltaics,* vol. 10, no. 5, pp. 1474-1480, 2020, doi: 10.1109/JPHOTOV.2020.3006994.

[41] N. A. Kelly and T. L. Gibson, "Increasing the solar photovoltaic energy capture on sunny and cloudy days," *Solar Energy,* vol. 85, no. 1, pp. 111-125, 2011/01/01/ 2011, doi: https://doi.org/10.1016/j.solener.2010.10.015.

[42] I. Muñoz, A. Guinda, G. Olivares, S. Díaz, A. M. Gracia-Amillo, and L. Casajús, "Evaluation of Horizontal Single-Axis Solar Tracker Algorithms in Terms of Energy Production and Operational Performance," *Solar RRL,* vol. 8, no. 1, p. 2300507, 2024, doi: https://doi.org/10.1002/solr.202300507.

[43] K. Rahbar, S. Eslami, R. Pouladian-Kari, and L. Kirchner, "3-D numerical simulation and experimental study of PV module self-cleaning based on dew formation and single axis tracking," *Applied Energy,* vol. 316, p. 119119, 2022/06/15/ 2022, doi: https://doi.org/10.1016/j.apenergy.2022.119119.

[44] J. E. Ramírez, "Harnessing Smart Solar Tracking: Advanced Algorithms for Hail Protection," in "Soltec Whitepaper," 2023. [Online]. Available: https://soltec.com/uploads/2023/11/Whitepaper-Hail-1.pdf

[45] K. Whitfield, "Extreme Weather Update: Greater Understanding Leads to Improved Risk Mitigation Strategies," in "Nextracker report," 2022. [Online]. Available: https://www.nextracker.com/blog/energy-insights/extreme-weather-update-greater-understanding-leads-to-improved-risk-mitigation-strategies/

[46] R. W. Andrews and J. M. Pearce, "The effect of spectral albedo on amorphous silicon and crystalline silicon solar photovoltaic device performance," *Solar Energy,* vol. 91, pp. 233-241, 2013/05/01/ 2013, doi: https://doi.org/10.1016/j.solener.2013.01.030.

[47] N. P. Harder *et al.*, "Position Dependence of the Performance Gain by Selective Ground Albedo Enhancement for Bifacial Installations," in *2023 IEEE 50th Photovoltaic Specialists Conference (PVSC)*, 11-16 June 2023 2023, pp. 1-6, doi: 10.1109/PVSC48320.2023.10359920.

[48] M. R. Lewis, S. Ovaitt, B. McDanold, C. Deline, and K. Hinzer, "Energy Yield and Economics of Single-Axis-Tracked Bifacial Photovoltaics with Artificial Ground Reflectors," in *2023 IEEE 50th Photovoltaic Specialists Conference (PVSC)*, 11-16 June 2023 2023, pp. 1-1, doi: 10.1109/PVSC48320.2023.10360010.

[49] M. R. Lewis, S. Ovaitt, B. McDanold, C. Deline, and K. Hinzer, "Artificial ground reflector size and position effects on energy yield and economics of single-axis-tracked bifacial photovoltaics," *Progress in Photovoltaics: Research and Applications,* vol. n/a, no. n/a, 2024, doi: https://doi.org/10.1002/pip.3811.

[50] B. Marion, "Albedo Measurement of the Terra Pave White Albedo Product: Cooperative Research and Development Final Report, CRADA Number CRD-20-16729," National Renewable Energy Laboratory, 2021, vol. NREL/TP-5K00-80863.
[51] C. European, C. Joint Research, A. Chatzipanagi, N. Taylor, and A. Jaeger-Waldau, *Overview of the potential and challenges for agri-photovoltaics in the European Union*. Publications Office of the European Union, 2023.
[52] J. Macknick *et al.*, "The 5 Cs of Agrivoltaic Success Factors in the United States: Lessons from the InSPIRE Research Study," United States, 2022. [Online]. Available: https://www.osti.gov/biblio/1882930 https://www.osti.gov/servlets/purl/1882930
[53] H. J. Lee, H. H. Park, Y. O. Kim, and Y. I. Kuk, "Crop Cultivation Underneath Agro-Photovoltaic Systems and Its Effects on Crop Growth, Yield, and Photosynthetic Efficiency," *Agronomy,* vol. 12, no. 8, p. 1842, 2022. [Online]. Available: https://www.mdpi.com/2073-4395/12/8/1842.
[54] A. Kavga *et al.*, "Evaluating the experimental cultivation of peppers in low-energy-demand greenhouses. An interdisciplinary study," *Journal of the Science of Food and Agriculture,* vol. 99, no. 2, pp. 781-789, 2019, doi: https://doi.org/10.1002/jsfa.9246.
[55] B. Willockx, C. Lavaert, and J. Cappelle, "Performance evaluation of vertical bifacial and single-axis tracked agrivoltaic systems on arable land," *Renewable Energy,* vol. 217, p. 119181, 2023/11/01/ 2023, doi: https://doi.org/10.1016/j.renene.2023.119181.
[56] B. Valle *et al.*, "Increasing the total productivity of a land by combining mobile photovoltaic panels and food crops," *Applied Energy,* vol. 206, pp. 1495-1507, 2017/11/15/ 2017, doi: https://doi.org/10.1016/j.apenergy.2017.09.113.
[57] F. ISE. "HyPErFarm - Hydrogen and Photovoltaic Electrification on Farm." https://www.ise.fraunhofer.de/de/forschungsprojekte/hyperfarm.html (accessed April 28, 2024).
[58] F. ISE. "Modellregion Agri-PV BaWü." https://www.ise.fraunhofer.de/de/forschungsprojekte/agri-pv-bawue.html (accessed April 28, 2024).
[59] "Jack's Solar Garden." https://www.jackssolargarden.com (accessed April 28, 2024).
[60] NREL. "Agrivoltaics." https://www.nrel.gov/solar/market-research-analysis/agrivoltaics.html (accessed April 28, 2024).
[61] K. Ali Khan Niazi and M. Victoria, "Comparative analysis of photovoltaic configurations for agrivoltaic systems in Europe," *Progress in Photovoltaics: Research and Applications,* vol. 31, no. 11, pp. 1101-1113, 2023, doi: https://doi.org/10.1002/pip.3727.
[62] Z. Tahir and N. Z. Butt, "Implications of spatial-temporal shading in agrivoltaics under fixed tilt & tracking bifacial photovoltaic panels," *Renewable Energy,* vol. 190, pp. 167-176, 2022/05/01/ 2022, doi: https://doi.org/10.1016/j.renene.2022.03.078.
[63] F. J. Casares de la Torre, M. Varo, R. López-Luque, J. Ramírez-Faz, and L. M. Fernández-Ahumada, "Design and analysis of a tracking / backtracking strategy for PV plants with horizontal trackers after their conversion to agrivoltaic plants," *Renewable Energy,* vol. 187, pp. 537-550, 2022/03/01/ 2022, doi: https://doi.org/10.1016/j.renene.2022.01.081.
[64] D. Jung, G. H. Gareis, A. Staiger, and A. Salmon, "Effects of soiling on agrivoltaic systems: Results of a case study in Chile," *AIP Conference Proceedings,* vol. 2635, no. 1, 2022, doi: 10.1063/5.0107943.
[65] L. M. Cook and R. H. McCuen, "Hydrologic Response of Solar Farms," *Journal of Hydrologic Engineering,* vol. 18, no. 5, pp. 536-541, 2013, doi: doi:10.1061/(ASCE)HE.1943-5584.0000530.

[66] J. R. Caron and B. Littmann, "Direct monitoring of energy lost due to soiling on first solar modules in California," in *2012 IEEE 38th Photovoltaic Specialists Conference (PVSC) PART 2*, 3-8 June 2012 2012, pp. 1-5, doi: 10.1109/PVSC-Vol2.2012.6656732.

[67] J. Cano, J. J. John, S. Tatapudi, and G. TamizhMani, "Effect of tilt angle on soiling of photovoltaic modules," in *2014 IEEE 40th Photovoltaic Specialist Conference (PVSC)*, 8-13 June 2014 2014, pp. 3174-3176, doi: 10.1109/PVSC.2014.6925610.

[68] M. A. Sturchio *et al.*, "Grassland productivity responds unexpectedly to dynamic light and soil water environments induced by photovoltaic arrays," *Ecosphere,* vol. 13, no. 12, p. e4334, 2022, doi: https://doi.org/10.1002/ecs2.4334.

[69] Y. Elamri, B. Cheviron, A. Mange, C. Dejean, F. Liron, and G. Belaud, "Rain concentration and sheltering effect of solar panels on cultivated plots," *Hydrol. Earth Syst. Sci.,* vol. 22, no. 2, pp. 1285-1298, 2018, doi: 10.5194/hess-22-1285-2018.

[70] *IEC 61724-1: Photovoltaic system performance - Part 1: Monitoring*, IEC, 2021.

[71] M. Sengupta *et al.*, "Best Practices Handbook for the Collection and Use of Solar Resource Data for Solar Energy Applications," in "IEA Solar Heating and Cooling Program," 2015.

[72] M. Sengupta, A. Habte, S. Wilbert, C. Gueymard, and J. Remund, "Best Practices Handbook for the Collection and Use of Solar Resource Data for Solar Energy Applications," 2024, vol. Fourth Edition.

[73] M. Korevaar and D. Nitzel, "Simulation of POA Front Sensor Mounting," in *2023 European PVPMC*, Mendrisio, Switzerland, 2023, https://pvpmc.sandia.gov/workshops-and-pubs/workshops/2023-pvpmc-mendrisio/.

[74] D. Tschopp, A. R. Jensen, J. Dragsted, P. Ohnewein, and S. Furbo, "Measurement and modeling of diffuse irradiance masking on tilted planes for solar engineering applications," *Solar Energy,* vol. 231, 2022.

[75] M. Gostein *et al.*, "Measuring Irradiance for Bifacial PV Systems," presented at the 48th IEEE Photovoltaic Specialist Conference, 2021.

[76] J. L. Braid *et al.*, "Effective Irradiance Monitoring Using Reference Modules," presented at the IEEE 49th Photovoltaics Specialists Conference (PVSC), Philadelphia, 2022.

[77] N. Riedel-Lyngskær, M. Bartholomäus, J. Vedde, P. B. Poulsen, and S. Spataru, "Measuring Irradiance With Bifacial Reference Panels," *IEEE Journal of Photovoltaics,* vol. 12, no. 6, pp. 1324-1333, 2022, doi: 10.1109/JPHOTOV.2022.3201468.

[78] J. Polo, M. Alonso-Abella, A. Marcos, C. Sanz-Saiz, and N. Martín-Chivelet, "On the use of reference modules in characterizing the performance of bifacial modules for rooftop canopy applications," *Renewable Energy,* vol. 220, p. 119672, 2024/01/01/ 2024, doi: https://doi.org/10.1016/j.renene.2023.119672.

[79] *Solar energy — Specification and classification of instruments for measuring hemispherical solar and direct solar radiation*, I. 9060:2018, 2018.

[80] S. A. Pelaez, C. Deline, J. S. Stein, B. Marion, K. Anderson, and M. Muller, "Effect of torque-tube parameters on rear-irradiance and rear-shading loss for bifacial PV performance on single-axis tracking systems," in *2019 IEEE 46th Photovoltaic Specialists Conference (PVSC)*, 16-21 June 2019 2019, vol. 2, pp. 1-6, doi: 10.1109/PVSC40753.2019.9198975.

[81] S. Ovaitt, C. Deline, B. Sekulic, B. McDanold, J. Parker, and J. Stein, "Measuring and Modeling Bifacial Technologies," in *bifiPV 2022*, Konstanz, Germany, 2022.

[82] N. Riedel-Lyngskær and N. Andersen, "Strategies for Rear Irradiance Monitoring in Tracked Bifacial Systems," in *2023 PVPMC*, Salt Lake City, UT, 2023.

[83] C. Deline, M. Gostein, S. Ovaitt, J. Braid, J. Newmiller, and I. Suez, "Instrumenting Bifacial Fields for Capacity Testing and Modeling," in *bifiPV 2022*, Doha, 2023, doi: https://www.osti.gov/servlets/purl/2274800.

[84] N. Riedel-Lyngskær, M. Petit, D. Berrian, P. B. Poulsen, J. Libal, and M. L. Jakobsen, "A Spatial Irradiance Map Measured on the Rear Side of a Utility-Scale Horizontal Single Axis Tracker with Validation using Open Source Tools," in *2020 47th IEEE Photovoltaic Specialists Conference (PVSC)*, 15 June-21 Aug. 2020 2020, pp. 1026-1032, doi: 10.1109/PVSC45281.2020.9300608.

[85] C. W. Hansen, M. Farr, and L. Pratt, "Correcting bias in measured module temperature coefficients," in *2014 IEEE 40th Photovoltaic Specialist Conference (PVSC)*, 8-13 June 2014 2014, pp. 2651-2655, doi: 10.1109/PVSC.2014.6925475.

[86] R. Smith. (2015) Improving Long-Term Back-of-Module Temperature Measurements. *SolarPro*.

[87] J. Crimmins, K. McIntosh, L. Creasy, and K. Lee, "Field testing meets modeling: validated data on bifacial solar performance," in "Array Technologies White Paper," 2020.

[88] *IEC 60904-5: Photovoltaic devices - Part 5: Determination of the equivalent cell temperature (ECT) of photovoltaic (PV) devices by the open-circuit voltage method*, IEC, 2011.

[89] B. Stueve, "Eliminating Back-of-Module Temperature Sensors for Reference Modules Using Voc Temperature Measurement," in *10th PV Performance Modeling Collaborative (PVPMC) Workshop*, Albuquerque, 2018.

[90] K. Anderson, C. Downs, S. Aneja, and M. Muller, "A Method for Estimating Time-Series PV Production Loss From Solar Tracking Failures," *IEEE Journal of Photovoltaics,* vol. 12, no. 1, pp. 119-126, 2022, doi: 10.1109/JPHOTOV.2021.3123872.

[91] D. Ruth and M. Muller, "A methodology to analyze photovoltaic tracker uptime," *Progress in Photovoltaics: Research and Applications,* vol. 26, no. 7, pp. 491-501, 2018, doi: https://doi.org/10.1002/pip.3002.

[92] K. S. Anderson, C. W. Hansen, W. F. Holmgren, A. R. Jensen, M. A. Mikofski, and A. Driesse, "pvlib python: 2023 project update," *Journal of Open Source Software,* vol. 8, no. 92, p. 5994, 2023, doi: https://doi.org/10.21105/joss.05994.

[93] W. F. Holmgren, C. W. Hansen, and M. A. Mikofski, "pvlib python: a python package for modeling solar energy systems," *Journal of Open Source Software,* vol. 3, no. 29, p. 884, 2018.

[94] M. Gostein, B. Marion, and B. Stueve, "Spectral Effects in Albedo and Rearside Irradiance Measurement for Bifacial Performance Estimation," presented at the IEEE 47th Photovoltaic Specialist Conference (PVSC), Virtual, 2020.

[95] J. C. Blakesley, G. Koutsourakis, D. E. Parsons, N. A. Mica, S. Balasubramanyam, and M. G. Russell, "Sourcing albedo data for bifacial PV systems in complex landscapes," *Solar Energy,* vol. 266, p. 112144, 2023/12/01/ 2023, doi: https://doi.org/10.1016/j.solener.2023.112144.

[96] P. Merodio, F. Martínez-Moreno, R. Moretón, and E. Lorenzo, "Albedo measurements and energy yield estimation uncertainty for bifacial photovoltaic systems," *Progress in Photovoltaics: Research and Applications,* vol. 31, no. 11, pp. 1130-1143, 2023, doi: https://doi.org/10.1002/pip.3728.

[97] *Photovoltaic system performance – Part 1: Monitoring*, I. 61724-1:2021, 2021.

[98] J. Coakley, "Reflectance and Albedo, Surface," in *Encyclopedia of Atmos. Sciences*, 2003, pp. 1914–1923.

[99] A. Tuomiranta, P.-J. Alet, C. Ballif, and H. Ghedira, "Worldwide performance evaluation of ground surface reflectance models," *Solar Energy,* vol. 224, pp. 1063-1078, 2021/08/01/ 2021, doi: https://doi.org/10.1016/j.solener.2021.06.023.

[100] C. A. Gueymard, V. Lara-Fanego, M. Sengupta, and Y. Xie, "Surface albedo and reflectance: Review of definitions, angular and spectral effects, and intercomparison of major data sources in support of advanced solar irradiance modeling over the Americas," *Solar Energy,* vol. 182, pp. 194-212, 2019/04/01/ 2019, doi: https://doi.org/10.1016/j.solener.2019.02.040.

[101] M. T. Patel, M. R. Khan, A. Alnuaimi, O. Albadwawwi, J. J. John, and M. A. Alam, "Implications of Seasonal and Spatial Albedo Variation on the Energy Output of Bifacial Solar Farms: A Global Perspective," in *2019 IEEE 46th Photovoltaic Specialists Conference (PVSC)*, 16-21 June 2019 2019, pp. 2264-2267, doi: 10.1109/PVSC40753.2019.8981163.

[102] H. Darling and e. al., "Impacts of Albedo Estimation Method on Energy Estimates," in *2023 PVPMC Workshop*, Salt Lake City, UT, 2023.

[103] V. L. Fanego, "Annual Energy Production Uncertainty of Bifacial PV Plants Caused by Inaccuracies in Albedo Data: Case Studies Using SAM," in *2022 IEEE 49th Photovoltaics Specialists Conference (PVSC)*, 5-10 June 2022 2022, pp. 0923-0923, doi: 10.1109/PVSC48317.2022.9938944.

[104] D. Berrian and J. Libal, "A comparison of ray tracing and view factor simulations of locally resolved rear irradiance with the experimental values," *Progress in Photovoltaics: Research and Applications,* vol. 28, no. 6, pp. 609-620, 2020, doi: https://doi.org/10.1002/pip.3261.

[105] E. Lorenzo, "On the historical origins of bifacial PV modelling," *Solar Energy,* vol. 218, pp. 587-595, 2021/04/01/ 2021, doi: https://doi.org/10.1016/j.solener.2021.03.006.

[106] S. A. Pelaez and C. Deline, "bifacial_radiance: a python package for modeling bifacial solar photovoltaic systems," *Journal of Open Source Software,* vol. 5, no. 50, p. 1865, 2020, doi: https://doi.org/10.21105/joss.01865.

[107] A. R. Burgers, G. J. M. Janssen, and B. B. V. Aken, "BIGEYE: Accurate energy yield prediction of bifacial PV systems," presented at the 5th bifi PV Workshop, Denver, CO, 2018.

[108] A. J. Veldhuis and A. H. M. E. Reinders, "Real-Time Irradiance Simulation for PV Products and Building Integrated PV in a Virtual Reality Environment," *IEEE Journal of Photovoltaics,* vol. 2, no. 3, pp. 352-358, 2012, doi: 10.1109/JPHOTOV.2012.2189937.

[109] J. Robledo, J. Leloux, E. Lorenzo, and C. A. Gueymard, "From video games to solar energy: 3D shading simulation for PV using GPU," *Solar Energy,* vol. 193, pp. 962-980, 2019/11/15/ 2019, doi: https://doi.org/10.1016/j.solener.2019.09.041.

[110] J. Robledo, J. Leloux, B. Sarr, C. A. Gueymard, and A. Driesse, "Dynamic and visual simulation of bifacial energy gain for photovoltaic plants," presented at the 38th European Photovoltaic Solar Energy Conference and Exhibition (EU PVSEC), Online, 2021.

[111] M. Theristis *et al.*, "Blind photovoltaic modeling intercomparison: A multidimensional data analysis and lessons learned," *Progress in Photovoltaics: Research and Applications,* vol. 31, no. 11, pp. 1144-1157, 2023, doi: https://doi.org/10.1002/pip.3729.

[112] E. Martínez-García, E. B. Marigorta, J. P. Gayo, and A. Navarro-Manso, "Experimental determination of the resistance of a single-axis solar tracker to torsional galloping," *Structural Engineering and Mechanics,* vol. 78, no. 5, pp. 519-528, 2021.

[113] X. Zhang, W. Ma, Z. Zhang, L. Hu, and Y. Cui, "Experimental study on the interference effect of the wind-induced large torsional vibration of single-axis solar

tracker arrays," *Journal of Wind Engineering and Industrial Aerodynamics,* vol. 240, p. 105470, 2023/09/01/ 2023, doi: https://doi.org/10.1016/j.jweia.2023.105470.

ISBN 978-3-907281-62-8